AD-A059 711

AD

MEMORANDUM REPORT ARBRL-MR-02841

A COMPARISON BETWEEN THE EULERIAN, HYDRODYNAMIC COMPUTER CODE (BRLSC) AND EXPERIMENTAL COLLAPSE OF A SHAPED CHARGE LINER

TECHNICAL LIBRARY

J. T. Harrison

June 1978

US ARMY ARMAMENT RESEARCH AND DEVELOPMENT COMMAND
BALLISTIC RESEARCH LABORATORY
ABERDEEN PROVING GROUND, MARYLAND

Approved for public release; distribution unlimited.

DTIC QUALITY INSPECTED 8

19971002 171

Destroy this report when it is no longer needed.
Do not return it to the originator.

Secondary distribution of this report by originating or sponsoring activity is prohibited.

Additional copies of this report may be obtained from the National Technical Information Service, U.S. Department of Commerce, Springfield, Virginia 22161.

The findings in this report are not to be construed as an official Department of the Army position, unless so designated by other authorized documents.

The use of trade names or manufacturers' names in this report does not constitute indorsement of any commercial product.

UNCLASSIFIED

SECURITY CLASSIFICATION OF THIS PAGE *(When Data Entered)*

REPORT DOCUMENTATION PAGE		READ INSTRUCTIONS BEFORE COMPLETING FORM
1. REPORT NUMBER MEMORANDUM REPORT ARBRL-MR-02841	2. GOVT ACCESSION NO.	3. RECIPIENT'S CATALOG NUMBER
4. TITLE *(and Subtitle)* A Comparison between the Eulerian, Hydrodynamic Computer Code (BRLSC) and Experimental Collapse of a Shaped Charge Liner.		5. TYPE OF REPORT & PERIOD COVERED Final 6. PERFORMING ORG. REPORT NUMBER
7. AUTHOR(s) J. T. Harrison		8. CONTRACT OR GRANT NUMBER(s)
9. PERFORMING ORGANIZATION NAME AND ADDRESS USA Ballistic Research Laboratory (ATTN: DRDAR-BLT) Aberdeen Proving Ground, MD 21005		10. PROGRAM ELEMENT, PROJECT, TASK AREA & WORK UNIT NUMBERS RDT & E 1L161102AH43
11. CONTROLLING OFFICE NAME AND ADDRESS US Army Armament Research & Development Command US Army Ballistic Research Laboratory (DRDAR-BL) Aberdeen Proving Ground, MD 21005		12. REPORT DATE JUNE 1978 13. NUMBER OF PAGES 50
14. MONITORING AGENCY NAME & ADDRESS *(if different from Controlling Office)*		15. SECURITY CLASS. *(of this report)* UNCLASSIFIED 15a. DECLASSIFICATION/DOWNGRADING SCHEDULE

16. DISTRIBUTION STATEMENT *(of this Report)*

Approved for public release; distribution unlimited.

17. DISTRIBUTION STATEMENT *(of the abstract entered in Block 20, if different from Report)*

18. SUPPLEMENTARY NOTES

19. KEY WORDS *(Continue on reverse side if necessary and identify by block number)*

Hydrodynamic, calculations, shaped charge, Eulerian, experiments, elastic-perfectly plastic.

20. ABSTRACT *(Continue on reverse side if necessary and identify by block number)* (hib) The Ballistic Research Laboratory Shaped Charge (BRLSC) code is a two-dimensional, hydrodynamic, elastic - perfectly plastic, finite - difference, Eulerian numerical technique developed to simulate the collapse process of a shaped-charge liner. This code is one of a family of HELP codes. The results from the BRLSC code are compared with data from two experimental shaped-charge liner collapse studies. First, the collapse of a 43mm diameter copper liner, driven by a bare composition-B explosive, then a 105mm liner driven by an unconfined

(over)

DD FORM 1 JAN 73 1473 EDITION OF 1 NOV 65 IS OBSOLETE

UNCLASSIFIED

SECURITY CLASSIFICATION OF THIS PAGE *(When Data Entered)*

(20. Continued)

composition-B explosive.

These comparisons show excellent agreement with the collapse sequence, the jet-tip velocity, and liner collapse velocity; but the jet density is low in the simulation. Jet density is an important parameter in the jet formation process if strength effects and breakup are to be satisfactorily modeled.

This report also presents a calculated parametric study where equation-of-state forms are varied producing a distinct difference in the computation of the jet-tip velocity and jet density in the computer simulation.

The aim of this work is to present to the munitions designer the current state-of-the-art for future research.

TABLE OF CONTENTS

LIST OF ILLUSTRATIONS

LIST OF ILLUSTRATIONS (CONTINUED)

I. INTRODUCTION

For many years computer specialists have been trying to model physical phenomena by using hydrodynamic computer codes. One such phenomenon is the shaped charge liner collapse. This report is a comparison between a hydrodynamic computer code and experimental results of this phenomenon.

The hydrodynamic computer code used in this comparison is the BRLSC (Ballistic Research Laboratory Shaped Charge) code[1]. This code, a modified version of the HELP code[2], is Eulerian formulated; that is, a computational grid or coordinate system is fixed in the region of interest, and the flow variables are calculated for each cell in the grid as the specified material moves through the cells. This code was developed specifically for the solution of the shaped charge problem which is two-dimensional, unsteady, compressible flow. The BRLSC code was developed by System, Science, and Software, Inc. under contract with the Ballistic Research Laboratory (BRL).

The experimental results are from two shaped charge systems. The first system, refered to as the "43mm shaped charge or 43mm cone diameter", is a hollow, conical, copper liner, driven by a right circular cylinder of bare composition B explosive. The second system refered to as the "105mm shaped charge" is also a hollow, conical copper liner, driven by an unconfined, right circular cylinder of composition B explosive.

The comparisons will consist of various experimental results (such as early-time flash radiographs of the liner collapse, jet tip velocity, jet and collapse velocity distributions, and jet density and temperature measurements), and their relationship to theoretical computed data presented in graphical form. Another series of comparisons will be presented from a calculated parametric study concerned with the variations in the equations of state of both liner and explosive. A detailed analysis of the calculated results will also be presented.

The objective of this report is to present results which will show the warhead designer the accuracy with which the BRLSC code can predict the liner collapse and jet formation process.

---

[1] *M. L. Gittings, "BRLSC: An Advanced Eulerian Code for Predicting Shaped Charges, Volume I," Ballistic Research Laboratories Contract Report No. 279, December 1975. (AD #A023962).*

[2] *L. J. Hageman and J. M. Walsh, "HELP, A Multi-material Eulerian Program for Compressible Fluid and Elastic-Plastic Flows in Two Space Dimensions and Time, Volume I, "Ballistic Research Laboratories Contract Report No. 39, May 1971. (AD #726459).*

II. BRLSC CODE DESCRIPTION

BRLSC is a FORTRAN code which has evolved from the OIL[3] hydrodynamic code and developed over a 15 year period.

The system of partial differential equations which is solved by the code consists of the balance equations of mass, momentum, and energy written with respect to a coordinate system fixed in space (Eulerian). These equations along with an equation of state and a stress - strain relationship are sufficient for the numerical solution of the detonation of high explosive, shaped charge liner collapse, and jet formation.

BRLSC code is time dependent in two space dimensions with an option for either plane (x,y) coordinates or axisymmetric cylindrical (r,z) coordinates. The time increment is based on the Courant stability condition and the maximum sound speed, plus the particle velocity in the grid. The resulting numerical technique is an explicit, conditionally stable, finite-difference system which is used to integrate the governing equations.

Solutions to these shaped charge problems involve the motion of a metal liner, which is accelerated by the pressure loading from a detonating explosive. The gas-metal interface is separated by lines joining massless tracer particles. These particles move across the grid and locate the interfaces and free surfaces of each material. Consequently, a Lagrangian effect is introduced into the treatment of moving surfaces.

The BRLSC code, using the Von Mises yield condition, has as an option the treatment of material as being elastic - perfectly plastic. But for the results reported herein, the liner material is treated as being purely hydrodynamic.

Plotting programs have been developed by the author at BRL to display the voluminous data generated during a computer run. In those figures, as indicated, the tracer particles were used to outline the interfaces and free surfaces of the different materials. Since the problems reported here are axisymmetric, only half of the various fields are presented.

---

[3] *W. E. Johnson, "OIL, A Continous Two-Dimensional Eulerian Hydrodynamic Code", Gulf General Atomic, G AMD-5580 Revised, January 1965.*

III. COMPARISON BETWEEN BRLSC CODE RESULTS AND 43MM SHAPED CHARGE EARLY-TIME FLASH RADIOGRAPHS

Figure 1 is a line drawing of the 43mm shaped charge, that was used in this comparison. Figure 2 shows the early-time-flash radiographs of the liner collapse of this charge. These radiographs were made by Boyd Taylor of the Ballistics Research Laboratory (BRL).[4] It begins with the arrival of the detonation wave at the apex of the cone, and continues at 2.4, 3.8, 5.6, 6.5, 7.6, 14.6 μs. A final exposure was made at 20 μs. The simulated shaped-charge liner collapse sequence is depicted in Figure 3 at five discrete times. These five times agree with those of the radiograph at 3.8, 5.6, 6.5, 7.6 and 9.6 μs. However, the code calculations do not include all of the time sequences from the flash radiographs shown in Figure 2. The first radiograph, corresponding to 2.4 μs, is not presented because the jet is not clearly defined in the picture. Also, those radiographs whose times are greater than 9.7 μs were excluded because the computer run time became excessive. The simulated collapse sequence agrees very well with those of the flash radiographs with which we can make comparisons.

Figure 4 is a calculational plot of the BRLSC code's results of the velocity difference between the tip of the jet and the tail of the slug, as a function of time after the detonation wave hits the apex of the cone. This difference is depicted by the broken line, and hereafter will be referred to as "relative jet tip velocity." This figure demonstrates that after approximately 11.5 μs, the jet tip reaches a constant relative velocity of 6.54mm/μs.

Figure 5 shows a comparison between the calculations of the BRLSC code in Figure 4, and the measured distances between the jet tip and the slug apex as a function of time, as depicted in Figure 2.

The slope of the line passing through the flash-radiograph data points is a constant, 6.54. This slope is the relative velocity of the jet tip with respect to the slug's tail, 6.54mm/μs. This is in agreement with the calculations of the BRLSC code depicted in Figure 4.

However, this graph shows a difference of approximately 1 μs in the movement of the jet tip, between the BRLSC code's results and the measurements from the radiograph. This difference is a result of either a timing problem in the recording instruments, or numerical problems regarding equations-of-state for the explosive, the metal, or both. Later in this report, a study of equations-of-state will be presented.

[4] *Private Communications from B. Taylor, Ballistic Research Laboratory, Aberdeen Proving Grounds, Maryland.*

DIMENSIONS
A = 43 mm
B = 46 mm
C = 73 mm
D = 1.25 mm

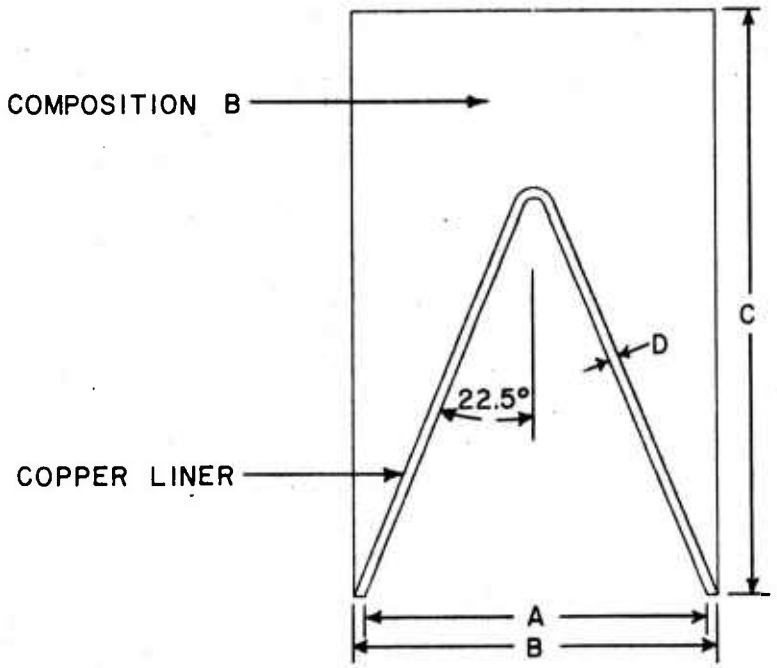

Figure 1. The line drawing of the 43mm shaped charge. Pertinent dimensions are shown in the table.

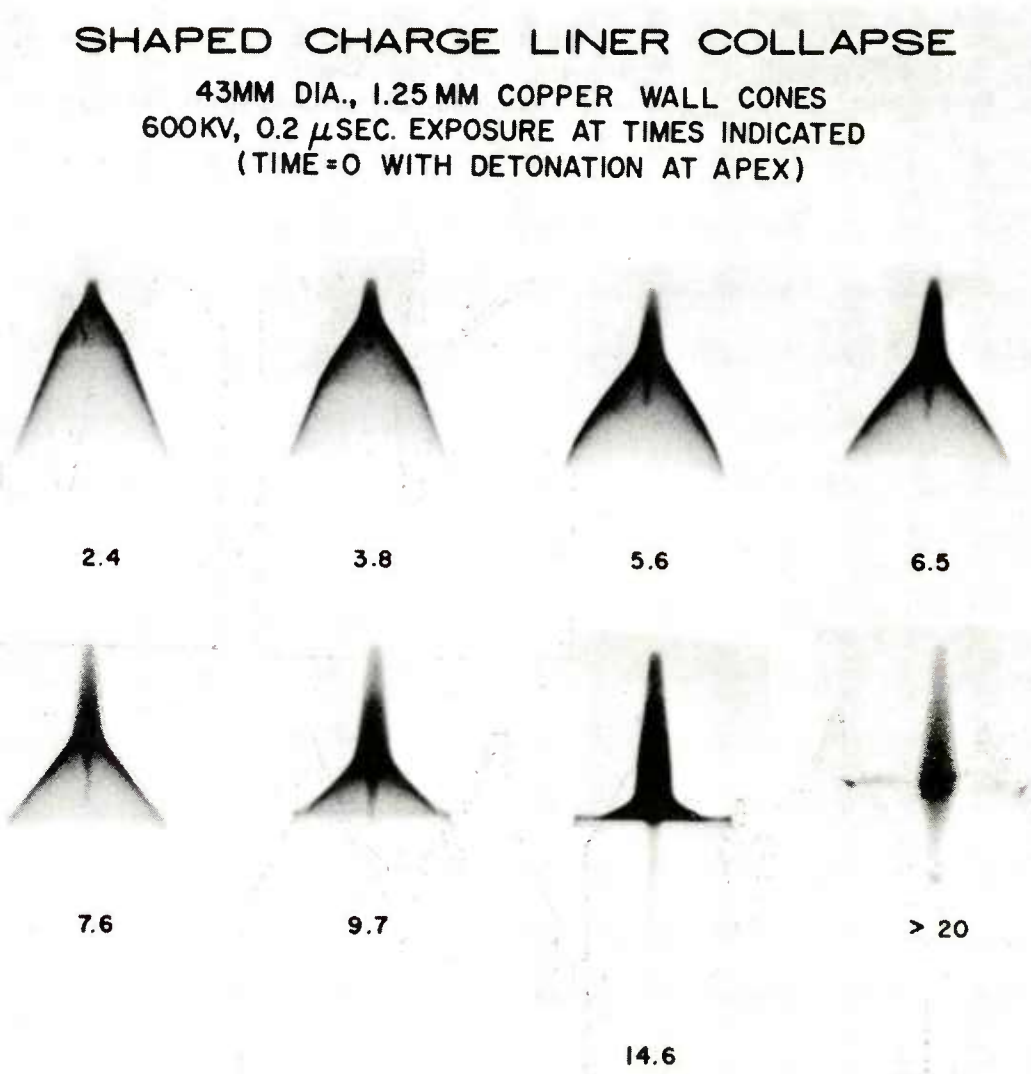

Figure 2. Experimental flash radiographs of the 43mm shaped charge liner collapse sequence. This figure is from reference 4. The unit of time is a microsecond.

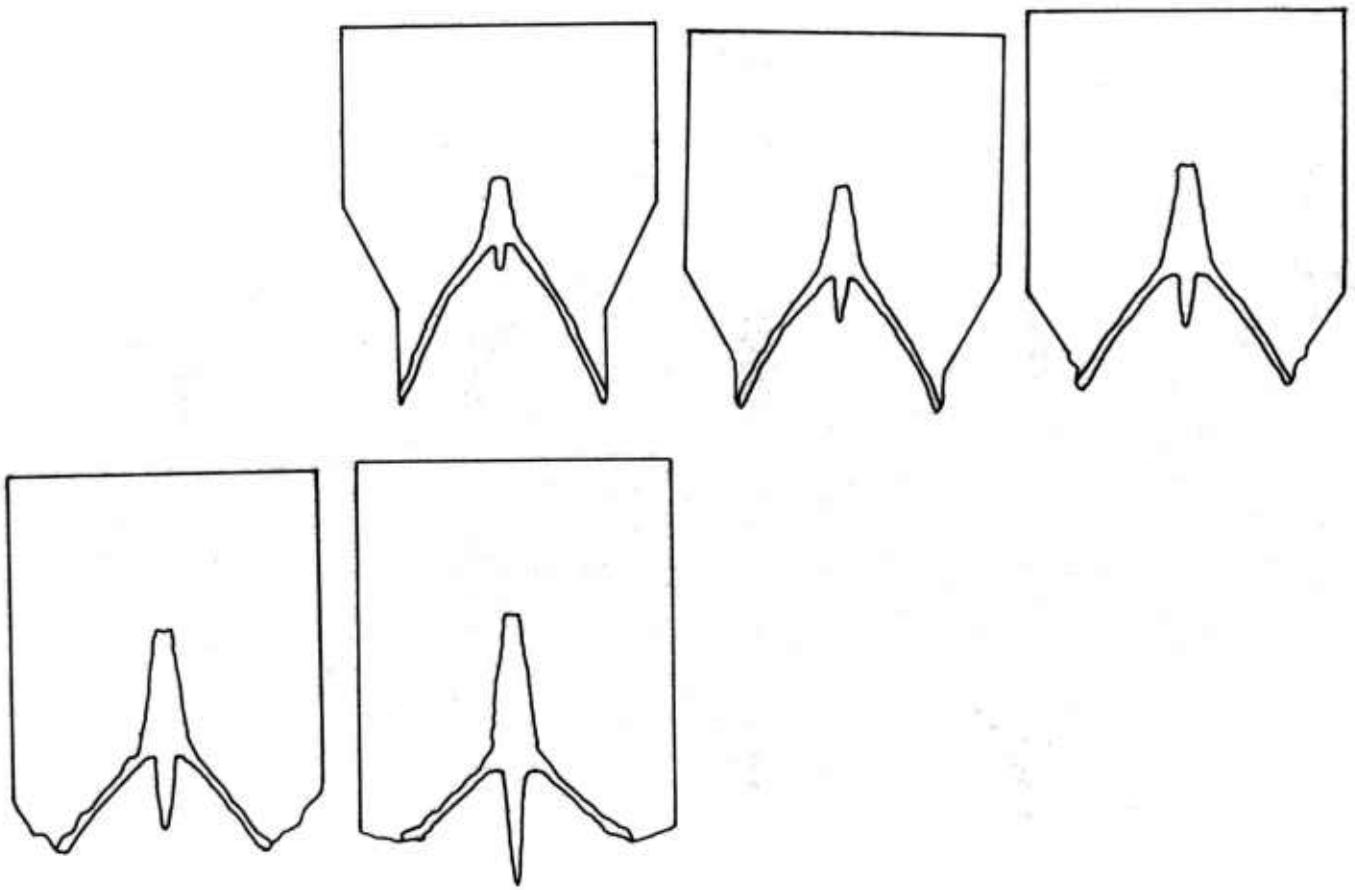

Figure 3. BRLSC code calculations depicting the 43mm, 1.25mm, copper wall, shaped charge liner collapse sequence. Times are 3.8, 5.6, 6.5, 7.6, and 9.7μs left to right and top to bottom respectively, with respect to Figure 2.

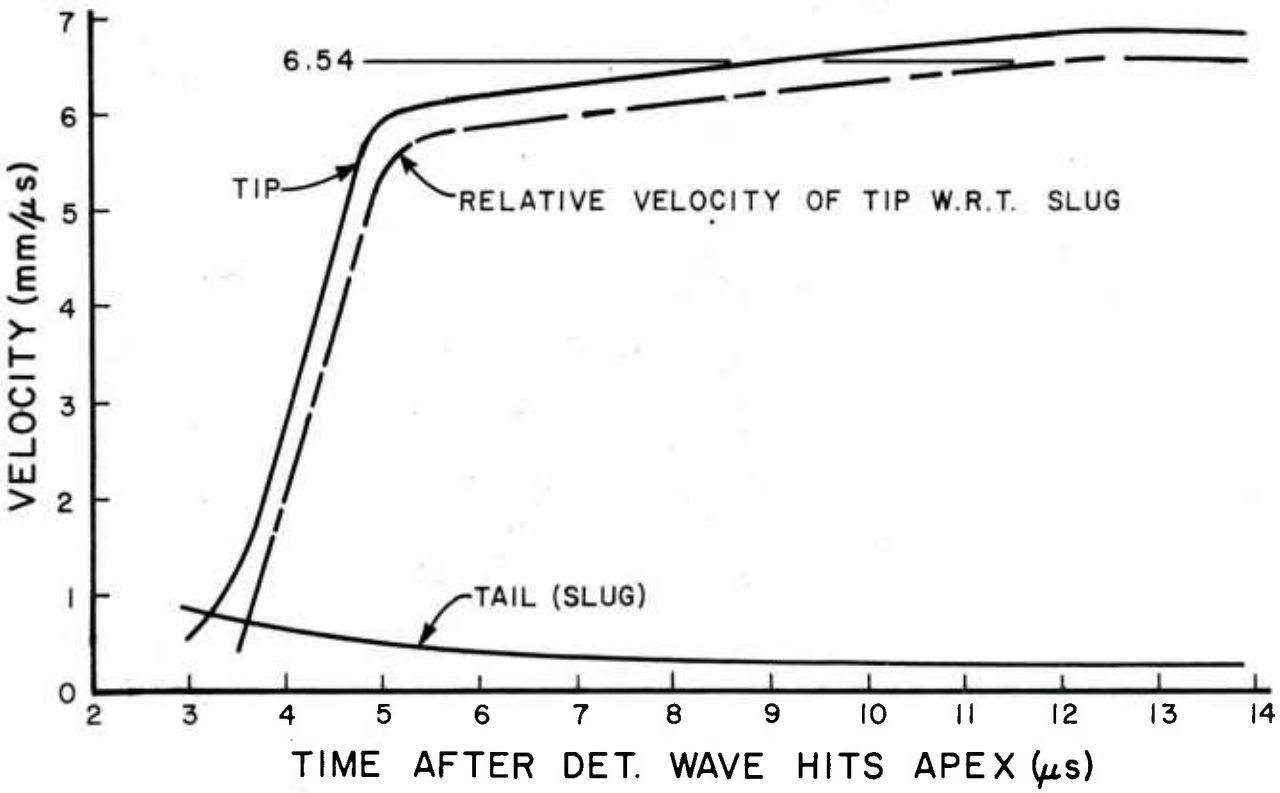

Figure 4. BRLSC code results from 43mm shaped charge calculations. The relative velocity of the jet tip with respect to tail (slug) is shown as the dashed line.

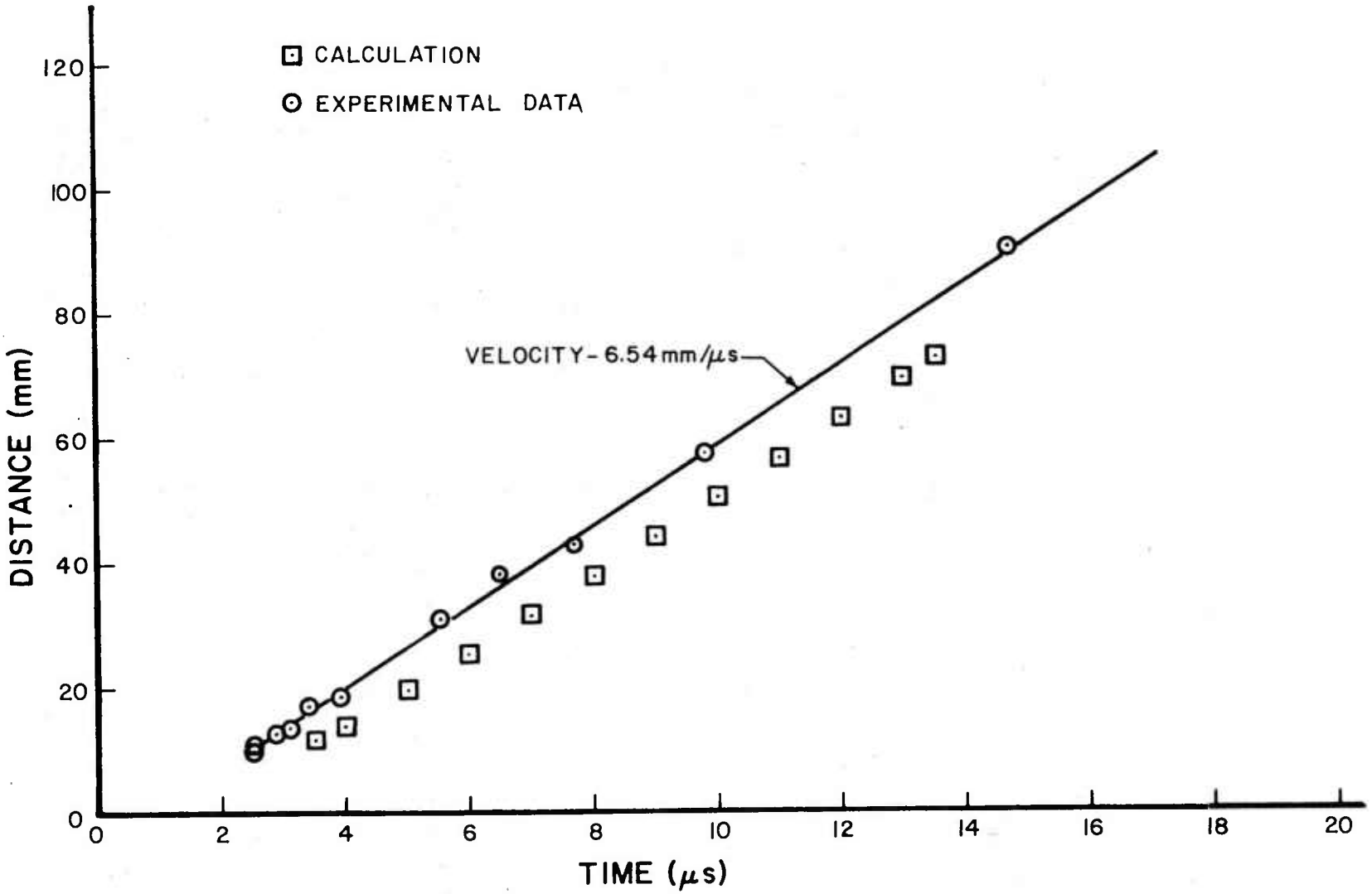

Figure 5. Comparison between the BRLSC code results and measured differences of the jet tip with respect to tail (slug), denoted by solid line taken from flash radiographs (Ref. 4)

Setting aside the small difference previously mentioned, one can conclude that the simulation is accurate on the basis of the aforementioned comparisons.

IV. DETAILED ANALYSIS OF THE CALCULATIONS FROM THE 43MM SHAPED CHARGE

The first graph in a detailed analysis of the 43mm shaped charge calculations, Figure 6, illustrates the axial component of velocity for liner material along the axis of symmetry as a function of axial distance. The time intervals of 8, 10, and 13μs are presented. The so called "inverse velocity gradient" in the jet is illustrated at the time intervals of 8 and 10 μs. This phenomena has been observed[5] and calculated[6] earlier by using a one-dimensional model of the shaped charge problem. This inverse velocity gradient in the jet is finally damped out by 13μs, and the jet tip is equilibrated to a velocity of approximately 6.8mm/μs.

The next graph in the analysis, Figure 7, contains three relations as functions of the axial position, for liner material, along the axis of symmetry. These three relations are ratios of density, ρ/ρ_o; specific internal energy, I/I_o; and pressure, P/P_o. Where the following are the normalizing units used in the above relationships as well as those in the remainder of this report unless otherwise stated:

a. $\rho_o = 8.9$ Mg/m^3

b. $I_o = 10^4$ joules/g

c. $P_o = 1.0$ Mbar.

In the vicinity of the jet tip, the density, Figure 7a, is 50% of the liner's initial density. The sublimation energy level, (I_s on the graph) Figure 7b, indicates that the calculated specific internal energy of the same region, i.e., jet tip, is six times greater. Also, eighty-three per cent of the liner material along the axis of symmetry has specific internal energy greater than I_s. This indicates the liner material has undergone vaporization, i.e. the expanded hot state, when $\rho/\rho_o < 1$ and $I > I'_s$ and transition state, when $\rho/\rho_o < 1$ and $I_s < I < I'_s$.

---

[5] *R. DiPersio and J. Simon, "An experimental Method of Obtaining Collapse Velocity of the Inner Walls of a Liner Shaped Charge Liner," Ballistic Research Laboratory Memorandum Report No. 1696, Aberdeen Proving Ground, MD, Sep 1965.* (AD #478326)

[6] *A. Kiwan and H. Wisniewski, "Theory and Computations of Collapse and Jet Velocities of Metallic Shaped Charge Liners," Ballistic Research Laboratory Report No. 1620, Aberdeen Proving Ground, MD, Nov 72.* (AD #907161)

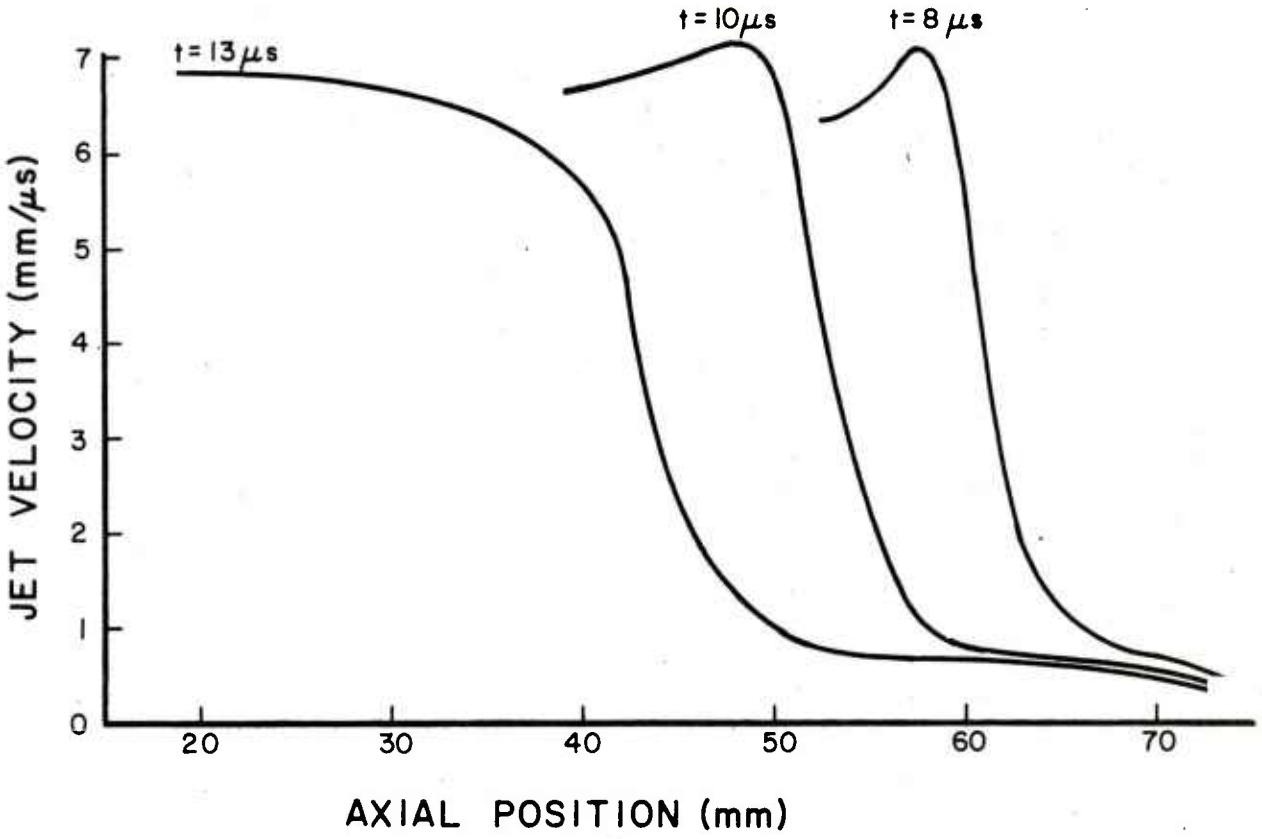

Figure 6. BRLSC code results of the axial velocity for the liner material along the axis of symmetry at 8, 10, and 13μs from the 43mm shaped charge with apex angle of 45°. The jet tip is on the left.

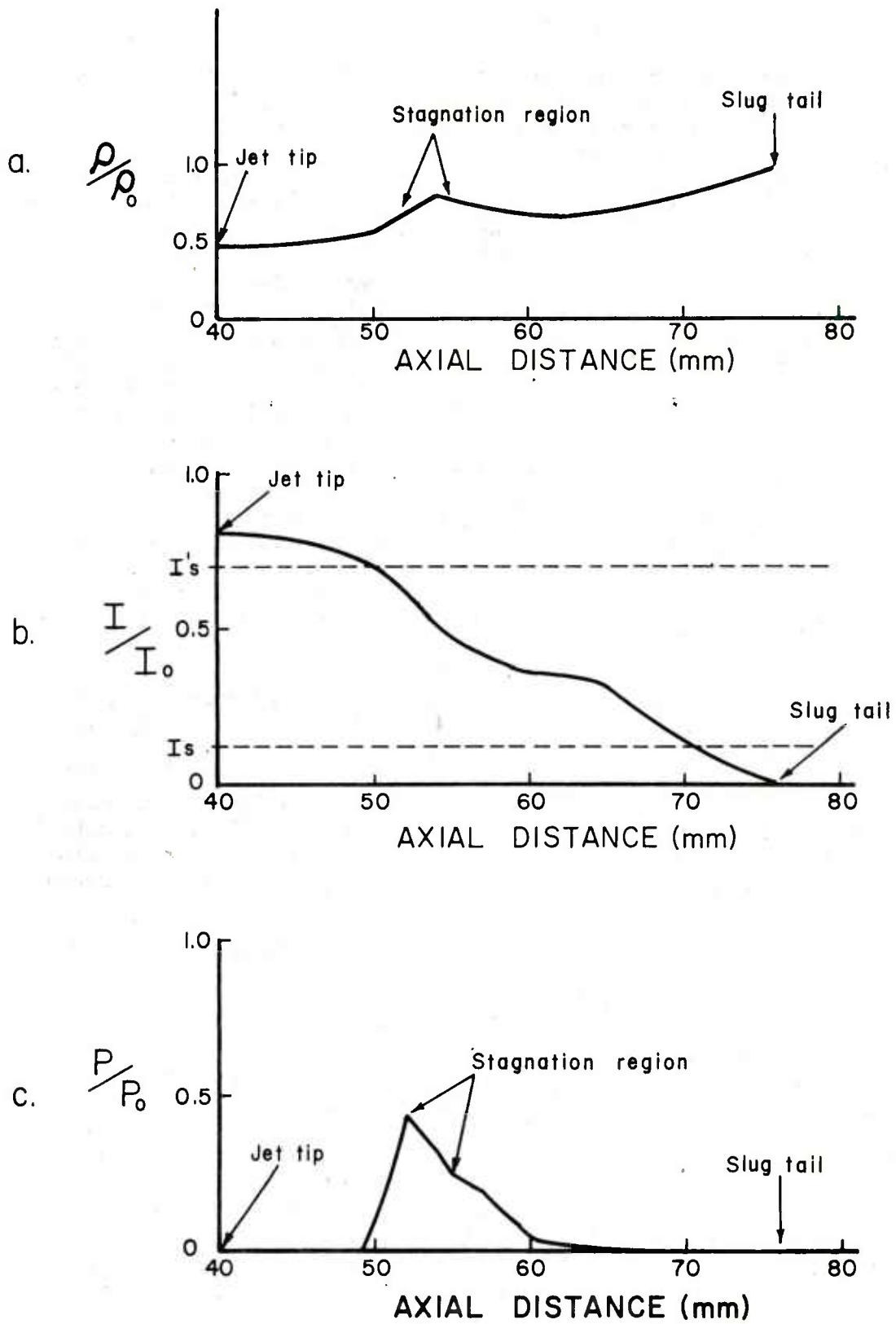

Figure 7. Detailed analysis of calculated results, of the 43mm shaped charge, along the axis of symmetry at 10μs after initiation of the explosive.

Interjected here are experimental observations regarding the continuous jet region, the leading pellet, for typical shaped charges. First, sample observations and densitometer measurements made from flash radiographs of the jet in free flight indicate that the density of the continuous jet is less than the initial density of the liner by about 15 to 20 percent.[7,8] This density corresponds to a temperature of 1500°C which is above the melting point of copper. Thus, the liquid state of the continuous jet is not ruled out, but these measurements do not take into account the possibility of voids along the jet's axis of symmetry which would result in lower density readings. Jamet claims that the jet breaks up in the solid state. Second, radiometry measurements of the jet's temperature were observed to be less than the melting point of the liner material.[9] These measurements were taken from both the side on and the front end view of the jet tip region. These experiments, conducted at the BRL, indicate that the continuous jet (tip) is cooler than the rest. Other experimental evidence[10] indicates that the tip region of the copper jet breaks up sooner than the following parts. The breakup time is faster for higher strength material[11] and the cooler jet tip would be expected to have more strength. Calculations show that the variation in temperature, from the jet elongation process, is negligible between jet formation and particulation.[11] The preponderant evidence indicates that the continuous jet tip is solid.

Figure 8 a, b, and c are the calculated results from the 43mm shaped charge depicting the ratio of density, ρ/ρ_o; ratio of specific internal energy, I/I_o; and jet velocity respectively for the jet tip as functions of time after the initiation of the explosive. Examining these three relationships we observe the following: first, the material density ratio goes thru a maximum compression with rapid acceleration and increase in specific internal energy for approximately 2μs; second,

---

[7] *Private communication from R. Jameson, Ballistic Research Laboratory, Aberdeen Proving Ground, MD.*

[8] *F. Jamet, "Mesure de la densit'e d'un jet de charge creuse en cuivre par radiographic - e'clair," Saint-Louis, Rapport - Bericht R 101/76, 9.1.1976.*

[9] *W. G. Von Holle and J. J. Trimble, "Temperature Measurement of Copper and Eutectic Metal Shaped Charge Jets," Ballistic Research Laboratory Report No. 2004, Aberdeen Proving Ground, MD, August 1977.* (AD #B021338L)

[10] *10P. C. Chou and J. Carleone, "Calculation of Shaped Charge Jet Strain, Radius and Breakup Time," BRL Contract Report CR246, July 1975, prepared by Dyna East Corp., Wynnewood, Pennsylvania. (AD#B0072406).*

[11] *R. R. Karpp and J. Simon, "An Estimate of the Strength of a Copper Shaped Charge Jet and the Effect of Strength on the Breakup of a Stretching Jet," BRL Report No. 1893, June 1976. (AD#B012141L)*

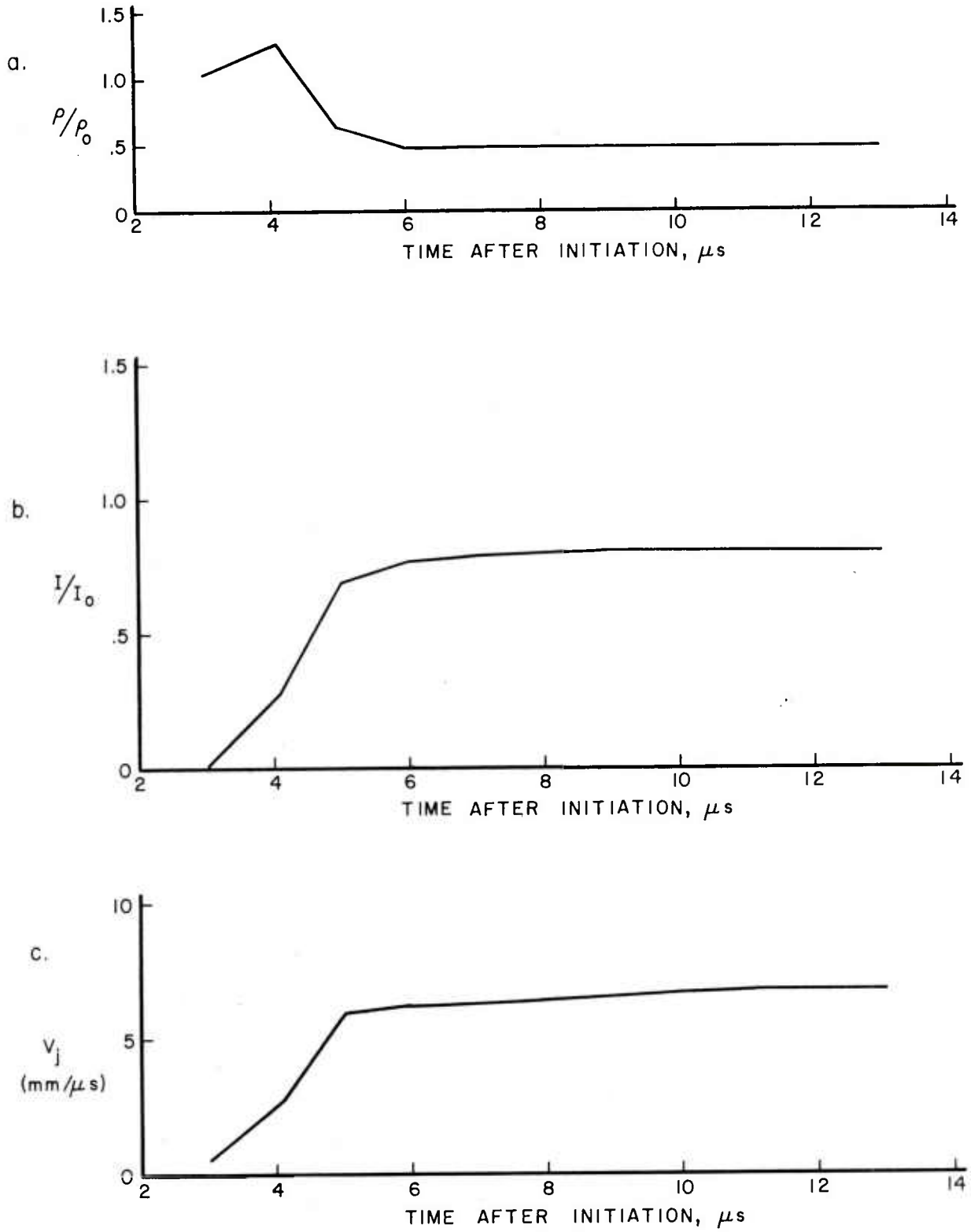

Figure 8. Detailed analysis of the 43mm shaped charge at the tip of the jet giving three functional relationships of time after the initiation of the explosive: a) density ratio, ρ/ρ_o; b) specific internal energy ratio I/I_o; c) axial velocity, V_j.

the material density ratio levels off to a constant with a gradual increase in specific internal energy and velocity while equilibrating the inverse velocity gradient for a period of approximately 5μs; and finally, steady flow.

V. 105MM SHAPED CHARGE ANALYSIS

The 105mm, unconfined shaped charge data[12] is a valuable source for comparing calculated results. Figure 9 a and b are the line drawings of the test charge and the initial configuration used in the BRLSC solution respectively. Several reports have been written regarding these data and various calculational techniques[13,14]. This report is the second effort to compare an Eulerian, two-dimensional, finite-difference, hydrodynamic calculational technique against these data. Comparisons between all currently existing calculated data and experimental results will be shown, as well as, calculated equations-of-state variations in a parametric study of this shaped charge.

Figure 10 illustrates the classical collapse and jet velocities as functions of relative distance from the apex of the cone. The respective final jet tip velocities of experiment and calculation are 7.0mm/μs and 6.8mm/μs. This demonstrates the major focal point of comparison between experimental and calculated results.

The procedure used in obtaining the calculated collapse and jet velocity data will be presented. First, the collapse velocity as a function of initial position along the liner, was obtained by monitoring the center line tracer at each time increment. As is illustrated in Figure 11, the center line tracer is the third tracer, from five tracers, denoted, as T_4 thru TO_4, initially spaced in even increments across the liner. The value of the collapse velocity depicted in Figure 10 is taken when this monitored tracer reaches its maximum as a function of time. Then the jet velocity, as a function of initial position along the liner, was obtained by monitoring the inside tracers, (for example, T_4 and T_5 in Figure 11), at each time

---

[12] *F. E. Allison and R. Vitali, "An application of the Jet-Formation Theory to a 105mm Shaped Charge," Ballistic Research Laboratories Report No. 1165, Aberdeen Proving Ground, MD, March 1961 (AD#277 458).*

[13] *M. L. Gittings, R. T. Sedgwick, and J. M. Walsh, "Numerical Analysis of Jet formation from Lined Shaped Charges," Ballistics Research Laboratories Contract Report No. 51, Aberdeen Proving Ground, MD, August 1971.* (AD #889631L)

[14] *J. T. Harrison and R. R. Karpp, "Terminal Ballistic Application of Hydrodynamic Computer Code Calculations," Ballistic Research Laboratory Report No. 1984, Aberdeen Proving Ground, MD, April 1977.* (AD #A041065)

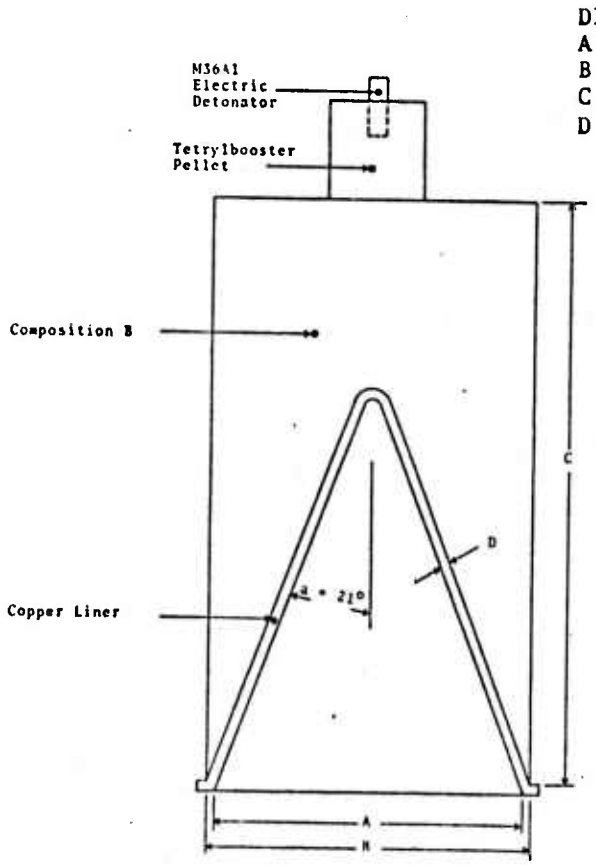

Figure 9a. The 105mm unconfined test charge used at the Ballistic Research Laboratory. Pertinent dimensions are shown in the table. This figure is from Ref. 12.

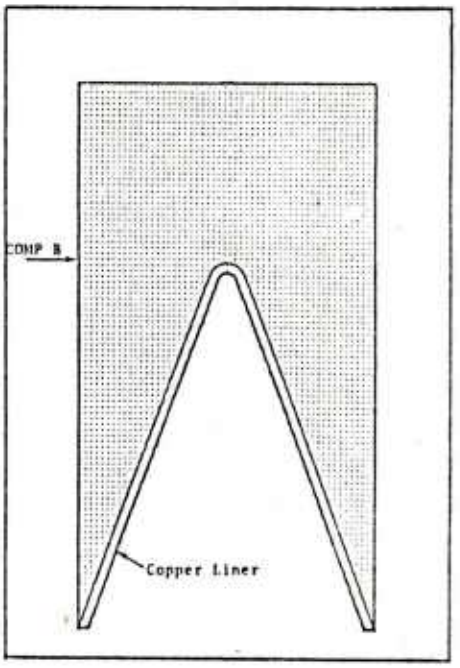

Figure 9b. Initial configuration used in BRLSC solution of the BRL-105mm unconfined test charge.

increment. Therefore, the calculated data contained on Figure 10 is the inside of the liner tracer's velocity distribution at the final computed time increment, which was 30μs after the initiation of the explosive. The calculation was terminated at that time increment due to initial grid boundary constraints. At this point, however, only approximately 45% of the initial liner had collapsed onto the axis of symmetry. The data is presented as it now stands. Collapse velocities were obtained from the entire liner since the detonation wave has traversed the liner at this time. Enough data are available to indicate that the calculated lead pellet or jet tip is projected from the first 18% of cone's distance from the apex, where as, experimental results show that the lead pellet emerged from the first 39% of the cone's distance from the apex. This difference is 45% of the experimental result. This is illustrated on Figure 10 as a constant jet velocity at the apex of the liner.

As another measure, we are able to compare the experimental and computed radial component of collapse velocity as a function of time after initiation of the explosive. This is illustrated on Figure 12 as the experimental, dashed lines, and computed, solid line. The experimental data were obtained by Randers-Pehrson[15]. These data points are on the inside surface of the liner at various initial radii positions monitored as a function of time after the initiation of the explosive. The computer code calculations are obtained by monitoring the inside passive tracer, for example T_4 and T_5 on Figure 11, as a function of time after the initiation of the explosive from which the radial component of the collapse velocity was extracted.

From the two Figures 10 and 12 we conclude that good agreement exists between the experimental and calculated collapse velocity distributions and that the jet velocity distributions are of the same general shape. We further conclude that good agreement was obtained between the experimental and calculated jet tip velocity with only a 3% variation but the calculated lead pellet's position from the apex of the cone is 45% of the experimental result.

VI. PARAMETRIC STUDY OF THE 105MM SHAPED CHARGE VARYING THE EQUATIONS-OF-STATE

The last study contained in this report is a parametric analysis of the 105mm, unconfined shaped charge with respect to the equation-of-state used in this calculational technique. Equations-of-state for both the metal liner and the explosive filler were varied parametrically.

---

[15]*Private Communication from G. Randers-Pehrson, Picatinny Arsenal, New Jersey.*

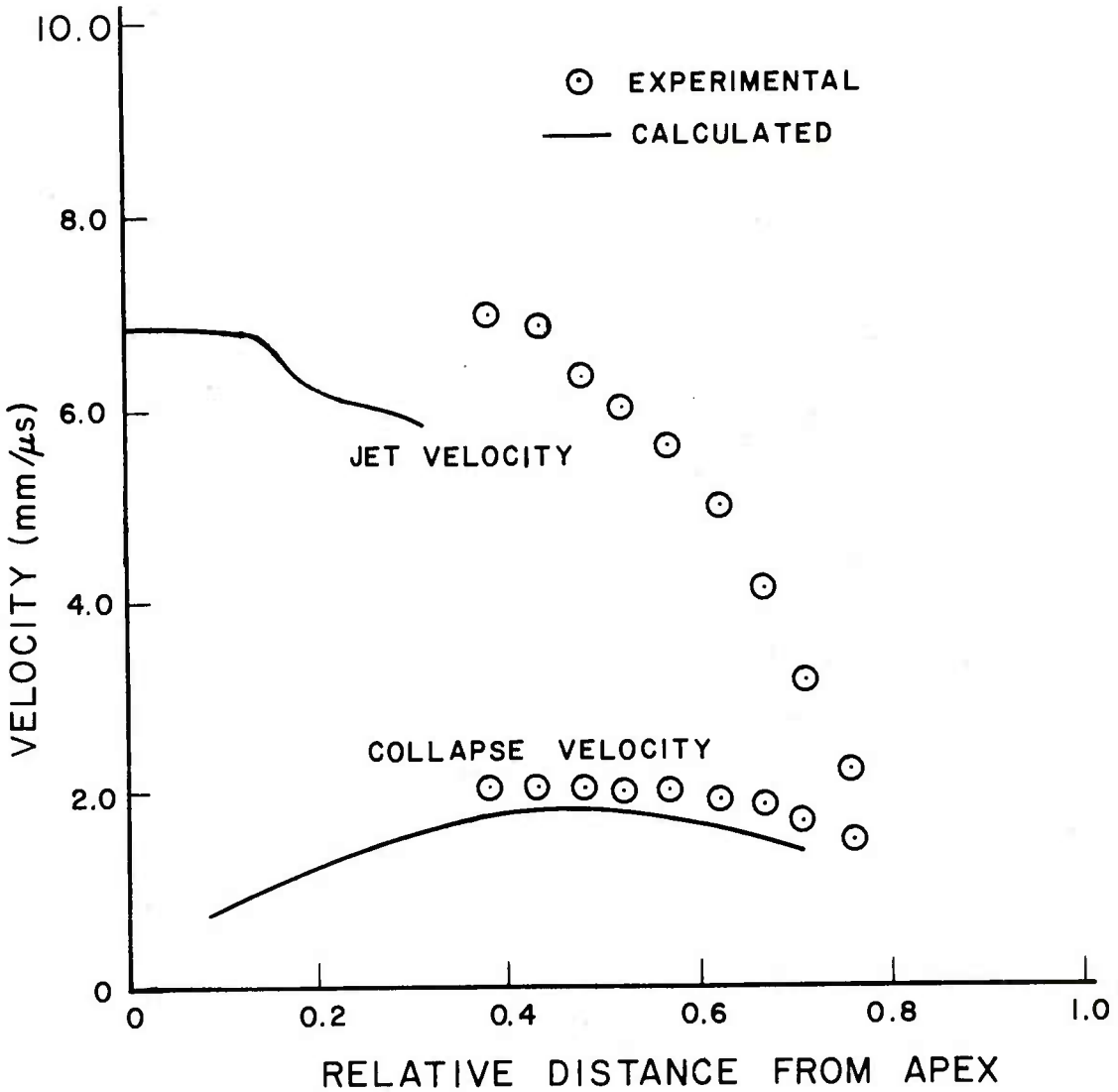

Figure 10. Comparison between experimental data from reference 12 and calculated collapse and jet velocity distributions from the 105mm shaped charge.

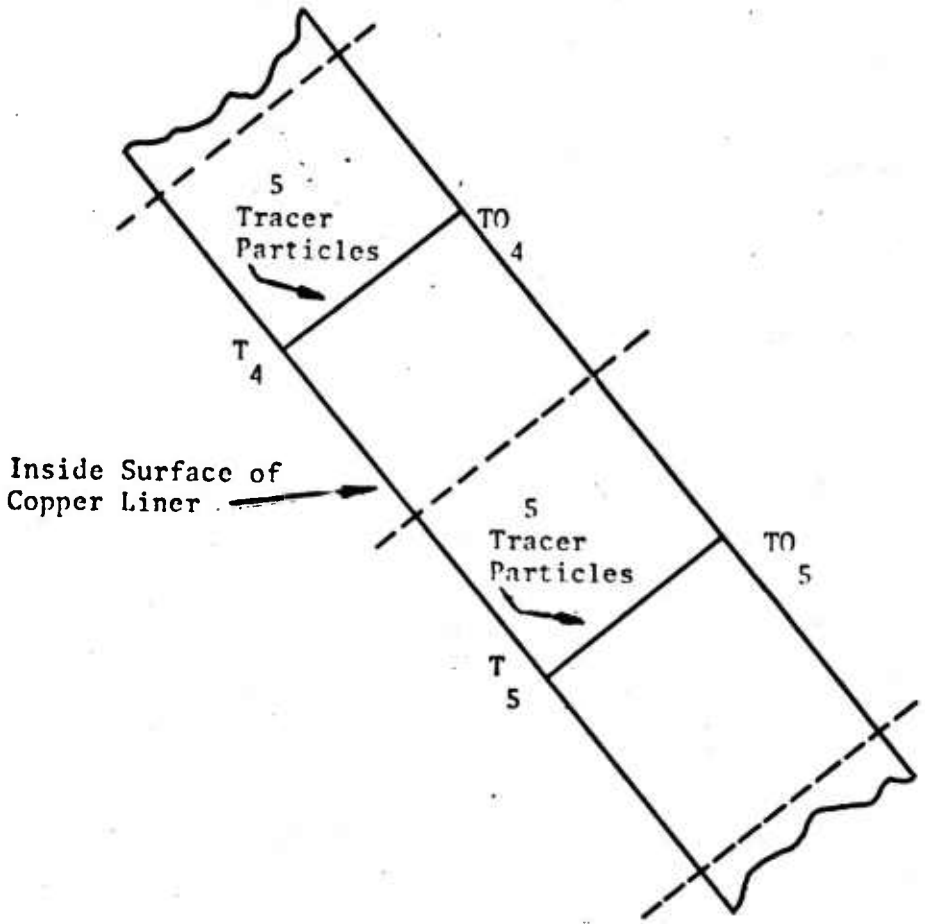

Figure 11. Section of copper liner showing the string of passive tracer particles employed for predicting collapse and jel velocity results.

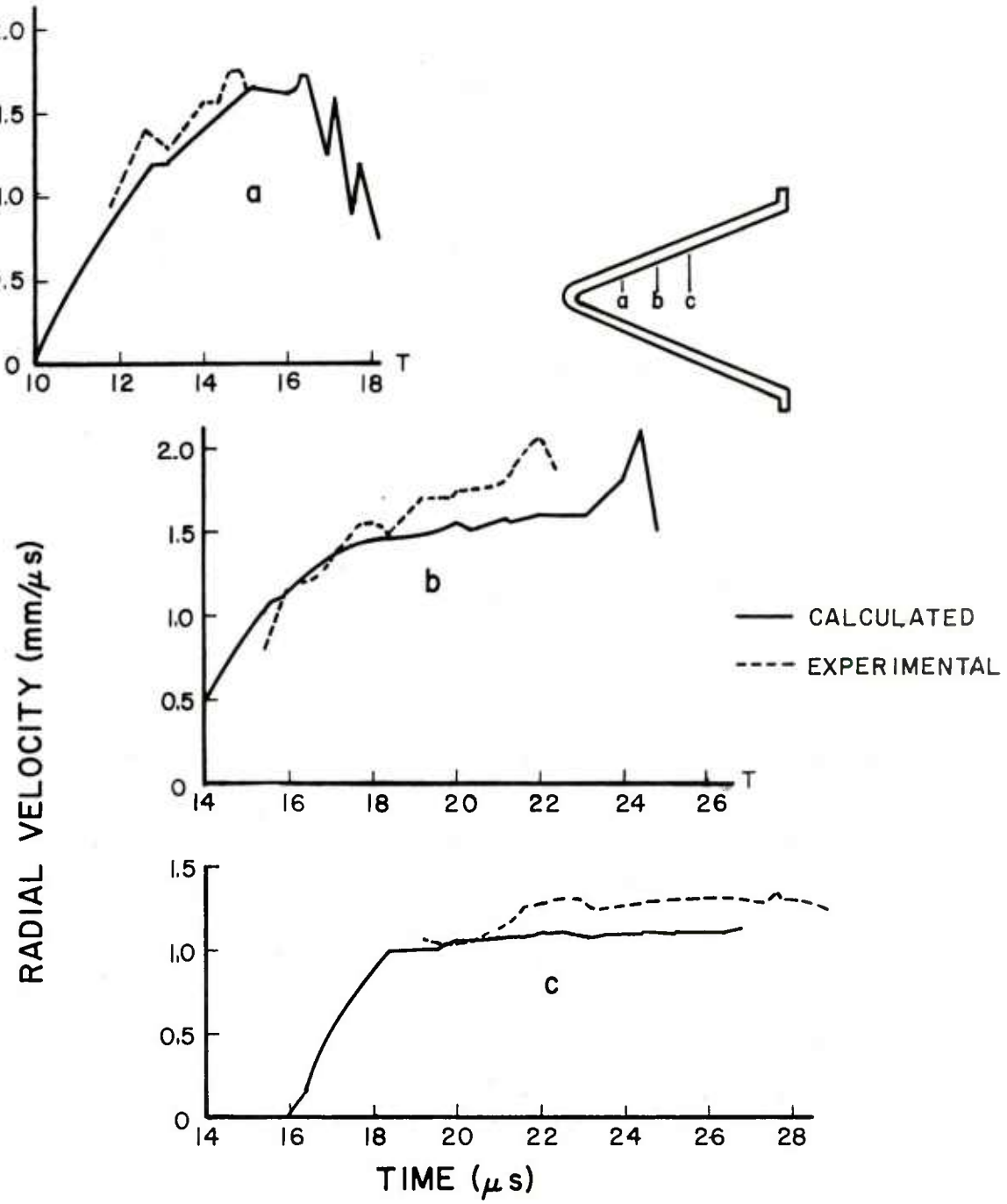

Figure 12. Comparison between experimental data from reference 15 and calculations of the radial collapse velocity from the 105mm shaped charge.

For clarity, the forms and constants of these state equations are presented as appendices to this report. The criteria utilized for the comparison are correlation of the jet tip velocity to the observed value of 7.0mm/μs and the flow field's tracer particle outlines at 20μs after the initiation of the explosive.

Tabulated in Table 1 are both the variable names associated with each equation-of-state are their respective jet tip velocity results.

Table 1. Equations of State and Jet Tip Velocities

Variation Number	Equation of State Name H.E.	Metal Liner	Jet Tip Velocity (mm/μs)
1	γ LAW	HEMP	6.2
2	γ LAW	Tillotson	7.3
3	JWL	HEMP	6.0
4	JWL	Tillotson	6.8

Figures 13-16 are the flow field tracer particle outlines of boundaries corresponding to numbers 1-4 respectively in Table 1. Based upon the criteria for the comparison, variation number 4 was chosen as the set of state equations to represent the best approximation of the physical phenomenon. This set of state equations was utilized in the previous study, i.e. the 43mm shaped charge study. All plots resulting from the calculation of variation number 4 will be presented. The first series of plots, Figures 17-20, are the velocity fields at times of 0, 5, 10, and 20μs. The final series of plots, Figures 21-24 are the two-dimensional pressure fields at the same respective times as above.

Having shown that variation number 4 gave the best prediction of jet tip velocity, we will compare it to variation number 3, the worst tip velocity prediction, in more detail. The data for variation number 3 are taken from Figure 25 which shows the results of assuming a HEMP equation of state where $p=f(\rho)$. For variation number 4, Figure 26 shows the results for a Tillotson equation of state where $p=f(\rho, I)$.

Table 2 summarizes a comparison of the jet tip properties for variations number 3 and 4, giving the maximum and minimum values. It will illustrate the differences in the computed results due to the state equations.

Table 2. Detailed Analysis at the Jet Tip Giving Minimum and Maximum Values

Variation Number	P/P_o (a minimum)	Velocity (mm/μs) (a maximum)	ρ/ρ_o (a minimum)	I/I_o (a maximum)
3	$P=f(\rho)=0$	6.0	1.0	1.45
4	$P=f(\rho,I)=0$	6.8	.48	1.45

This table illustrates that when specific internal energy is used in the solution of the pressure equation, $P=f(\rho,I)$, the jet tip is 48% of the initial liner density. However, the jet tip is traveling at a velocity which is 97% of the observed value. This table also illustrates that by eliminating the calculated specific internal energy, i.e. the Hugoniot relationship, will result in a density that is equal to the initial liner density, but, the jet tip velocity is 86% of the observed value. As an aside, we note that the value of the specific internal energy ratio at the jet tip for these two calculations as well as for the other calculations in the parameteric study are the same. This value is 10.5 times greater than I_s/I_o.

VII. CONCLUSION AND SUMMARY

These comparisons show an excellent agreement between calculated and experimental results during liner collapse. Also, calculated jet and liner collapse velocities compare well with experiments. But, when different forms of equations-of-state were applied in the BRLSC code, variations occur in both the jet density and velocity. The specific internal energy seems to be the source of the variations in the calculations. If these hydrodynamic computer codes are ever going to be able to model the entire physical process with detail and accuracy, then additional groundwork must be accomplished. We suggest investigating the following:

a. Check the equations-of-state,

b. determine if the numerical scheme's zone size is responsible for the exaggerated over-thermalization of specific internal energy,

c. determine whether or not a new numerical scheme, i.e., a second order or possibly a simple modification to the existing scheme, will bring better results.

As mentioned earlier, these determinations must be made before we can proceed with more sophisticated investigations such as strength effects and jet breakup.

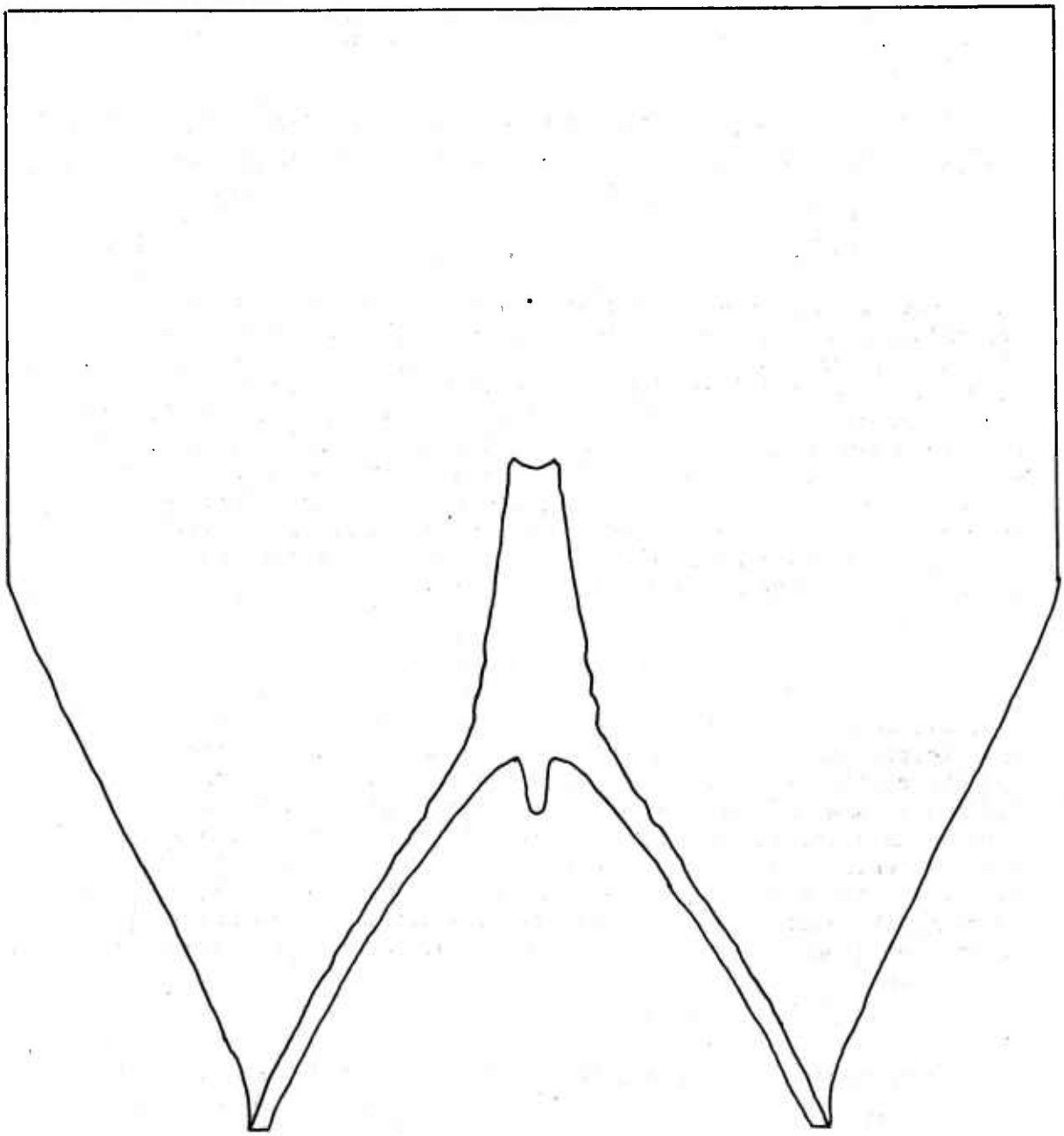

Figure 13. Computed flow field's tracer particle outlines of results from case number 1 on Table 1. Results are plotted at 20μs after initiation of the explosive.

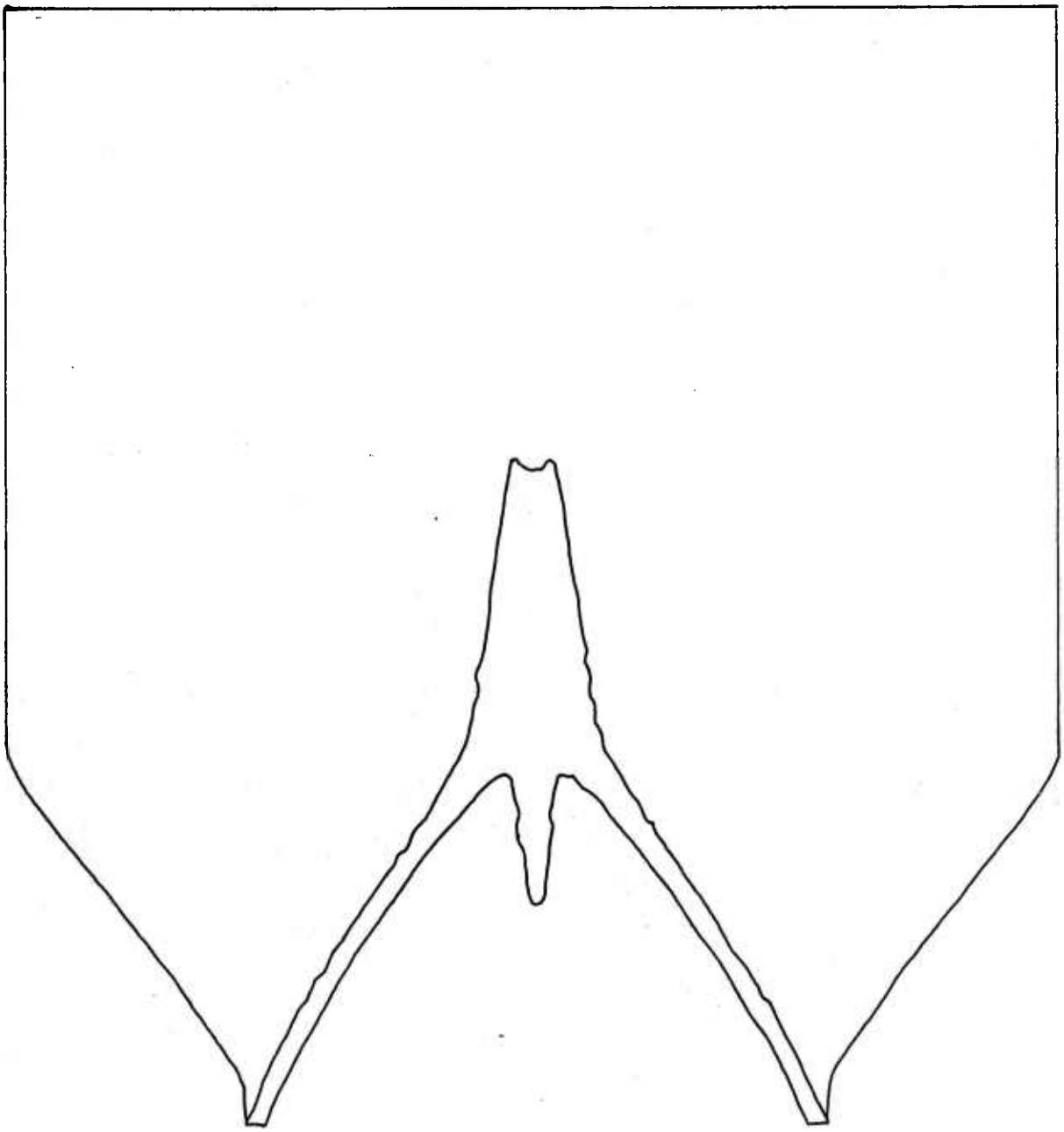

Figure 14. Computed flow field's tracer particle outlines of results from case number 2 on Table 1. Results are plotted at 20μs after initiation of the explosive.

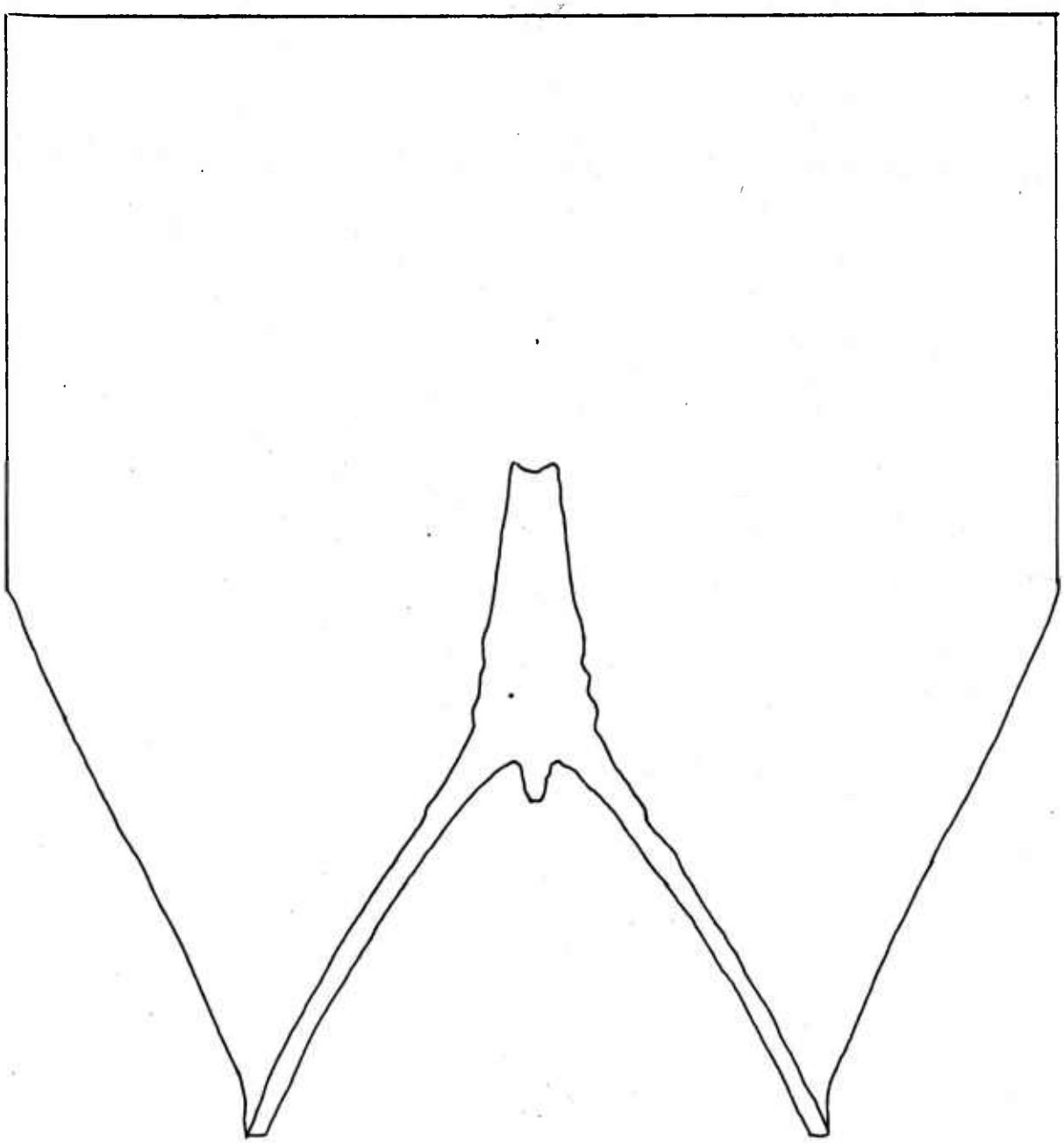

Figure 15. Computed flow field's tracer particle outlines of results from case number 3 on Table 1. Results are plotted at 20μs after initiation of the explosive.

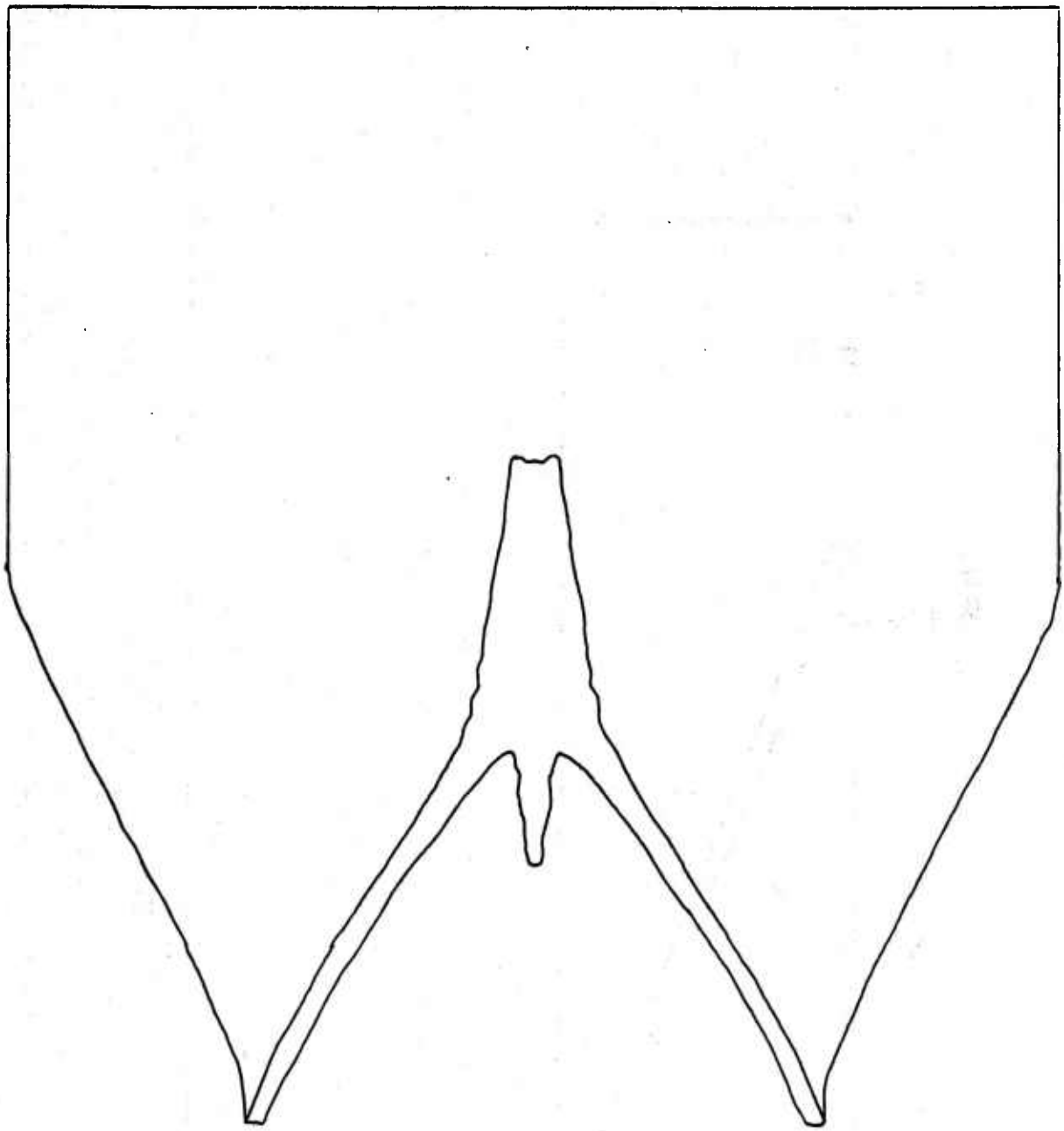

Figure 16. Computed flow field's tracer particle outlines of results from case number 4 on Table 1. Results are plotted at 20μs after initiation of the explosive.

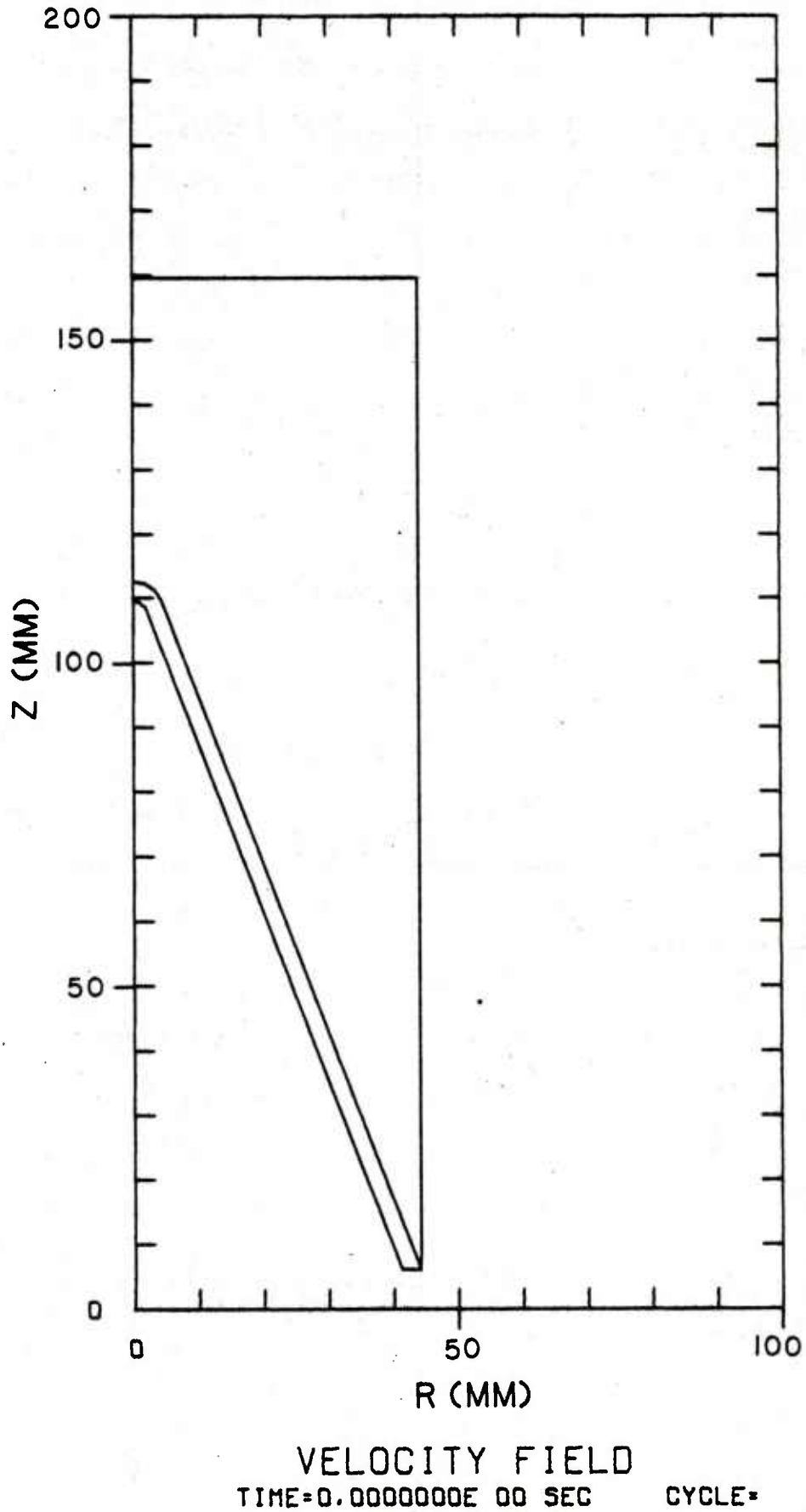

Figure 17. Velocity Field in the Eulerian grid at time = 0 μs. Results from number 4 on Table 1.

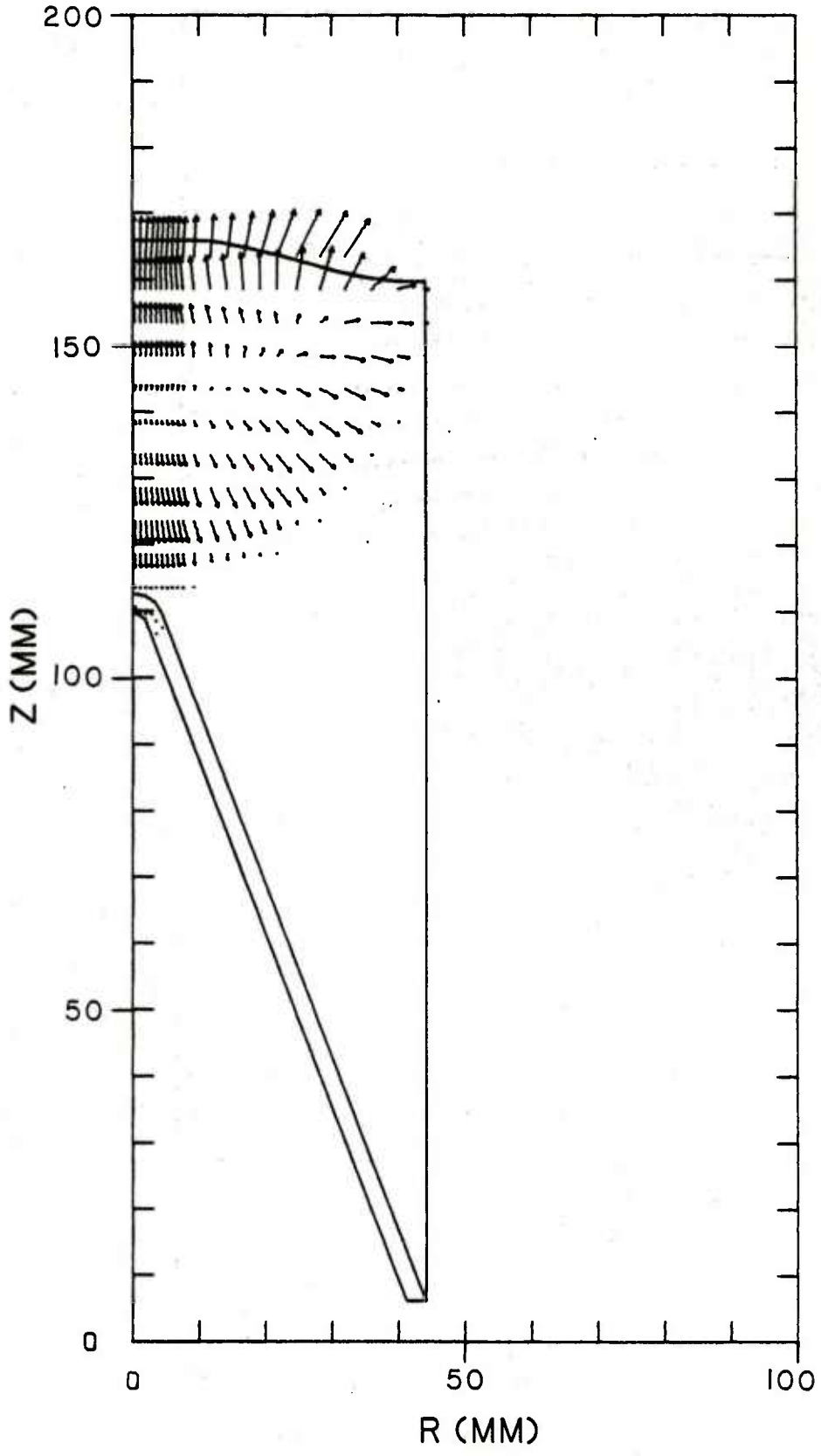

Figure 18. Velocity field on the Eulerian grid at time = 5μs. Results from run number 4 on Table 1.

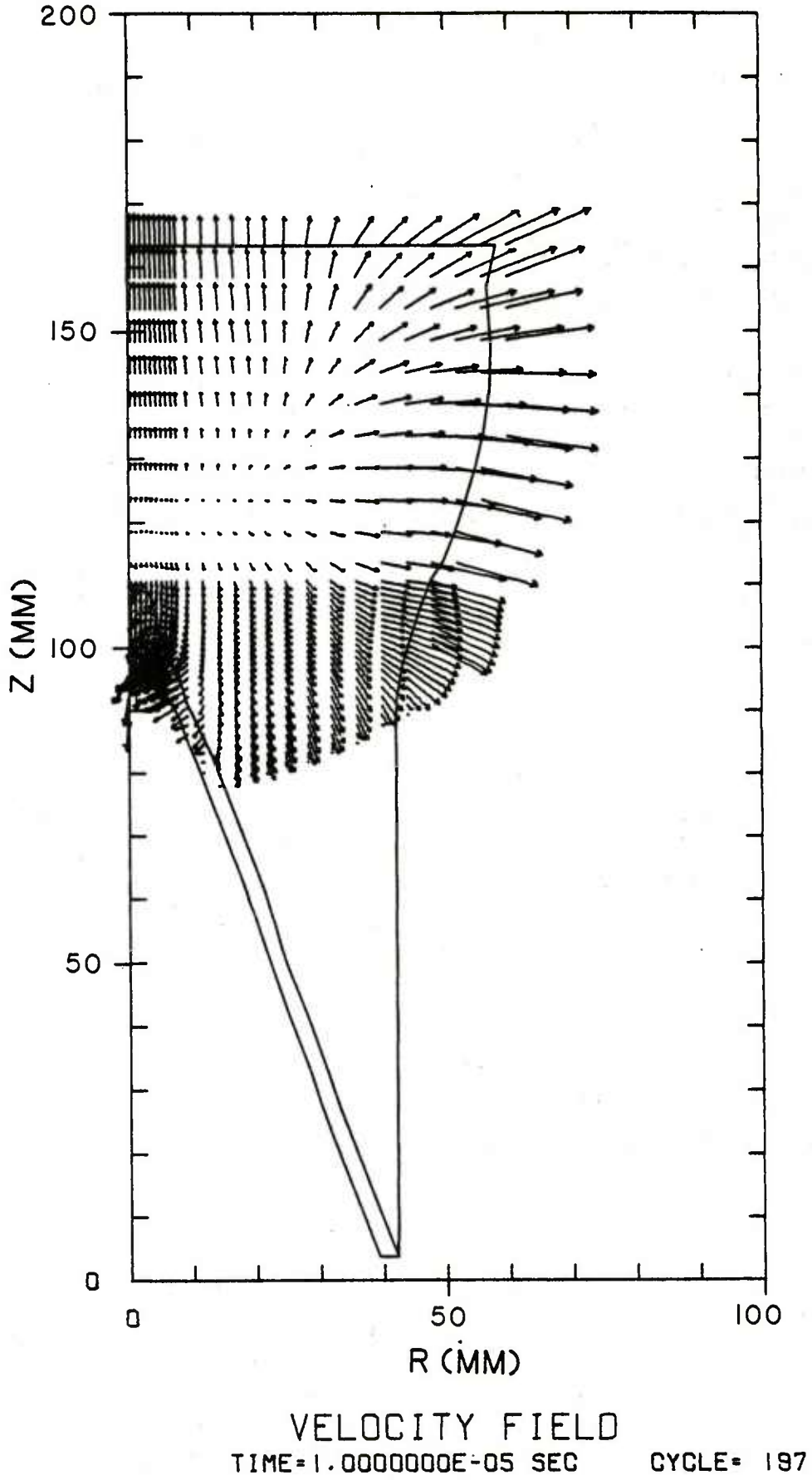

Figure 19. Velocity field on the Eulerian grid at time = 10μs. Results from run number 4 on Table 1.

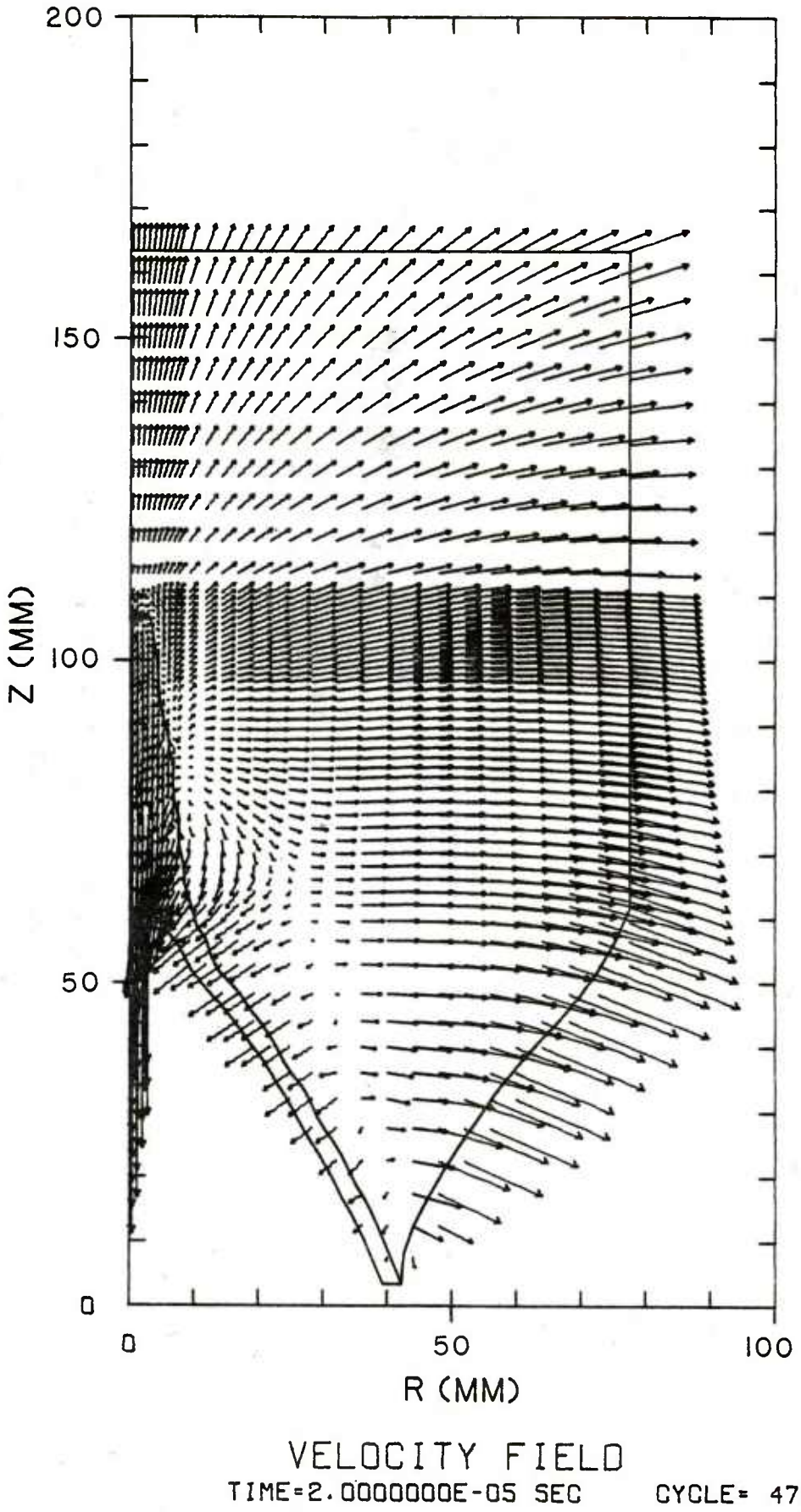

Figure 20. Velocity field on the Eulerian grid at time = 20μs. Results from run number 4 on Table 1.

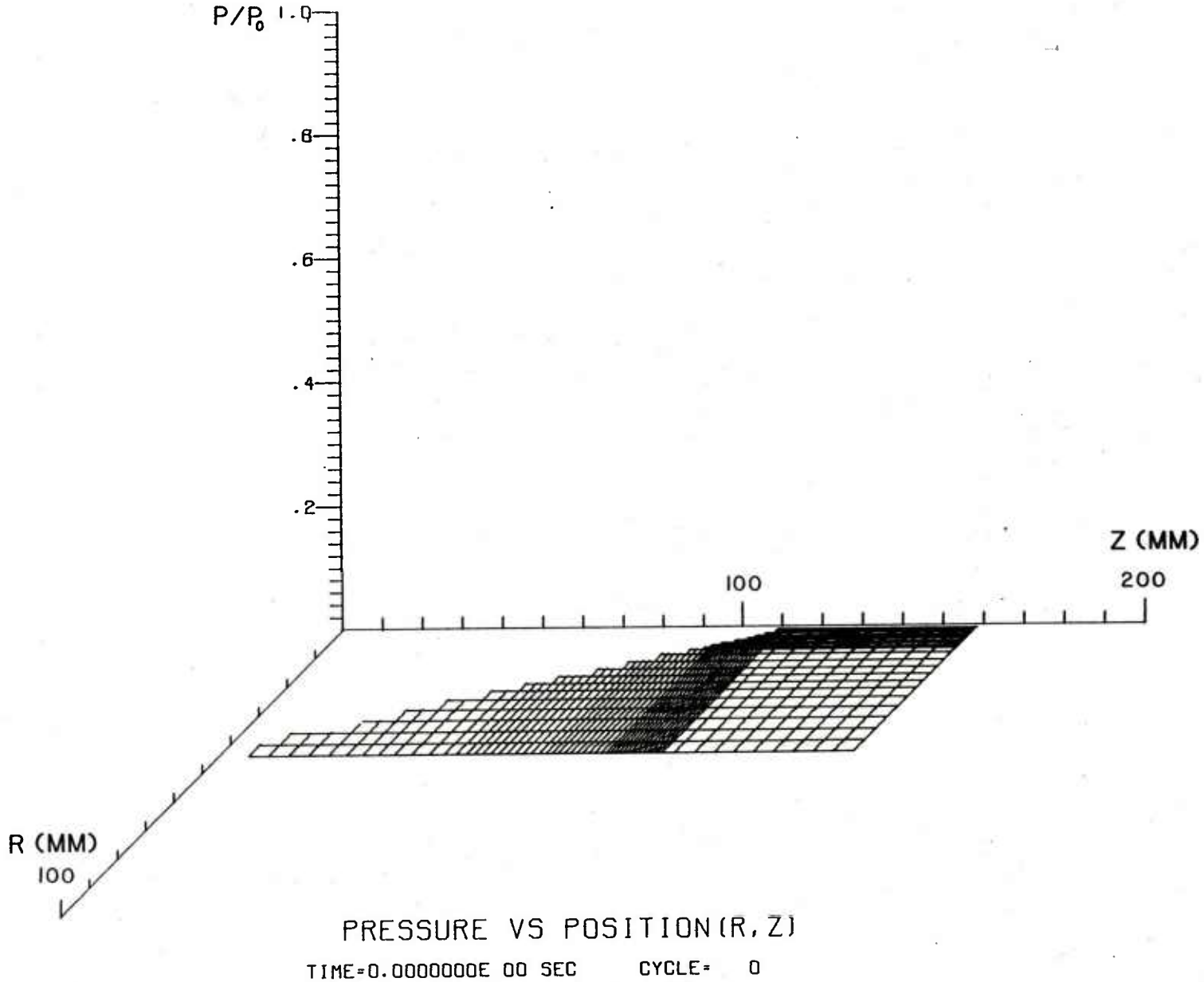

Figure 21. Three dimensional pressure field on the Eulerian grid at time = 0μs. Results from run number 4 on Table 1.

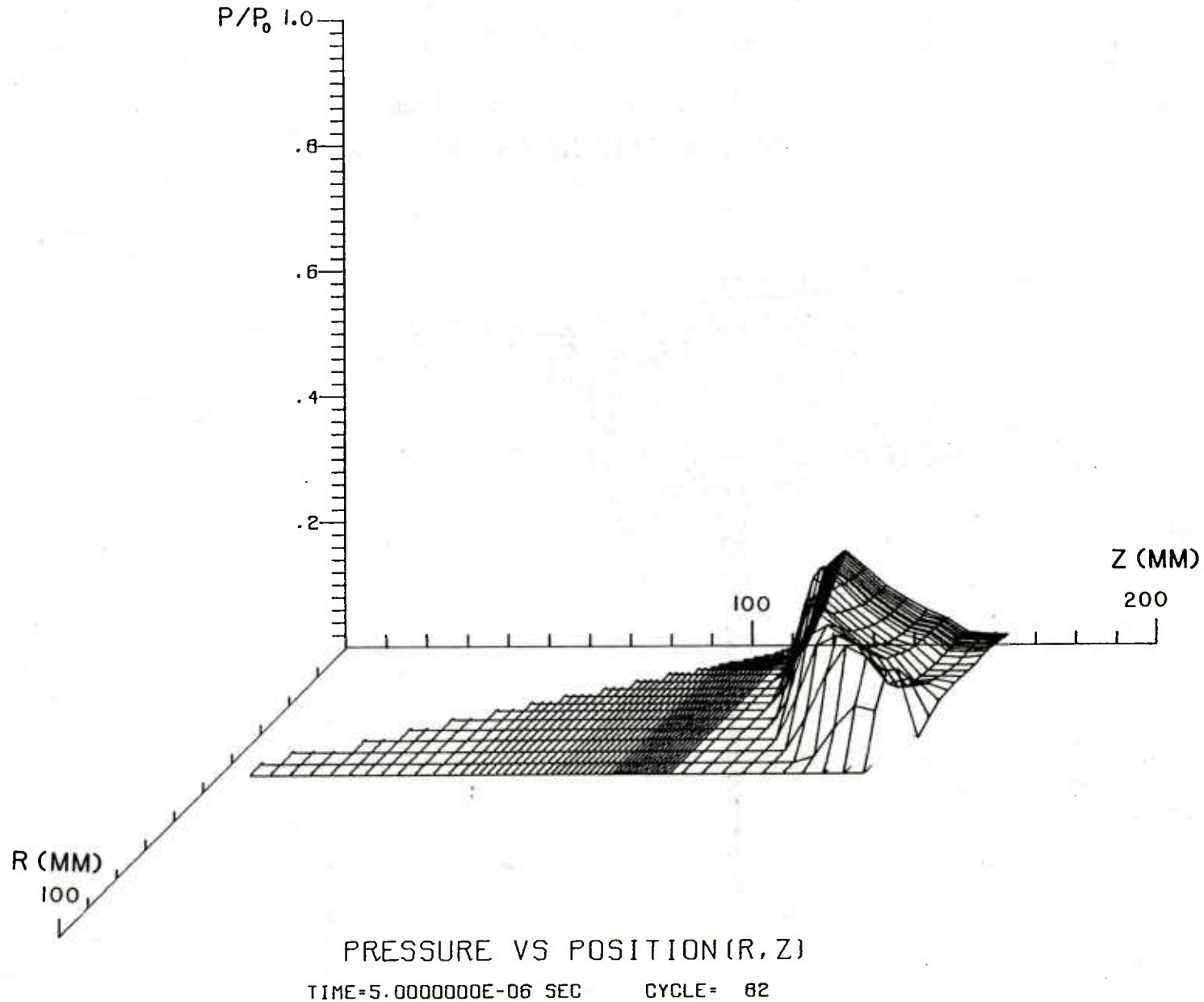

Figure 22. Three dimensional pressure field on the Eulerian grid at time = 5μs. Results from run number 4 on Table 1.

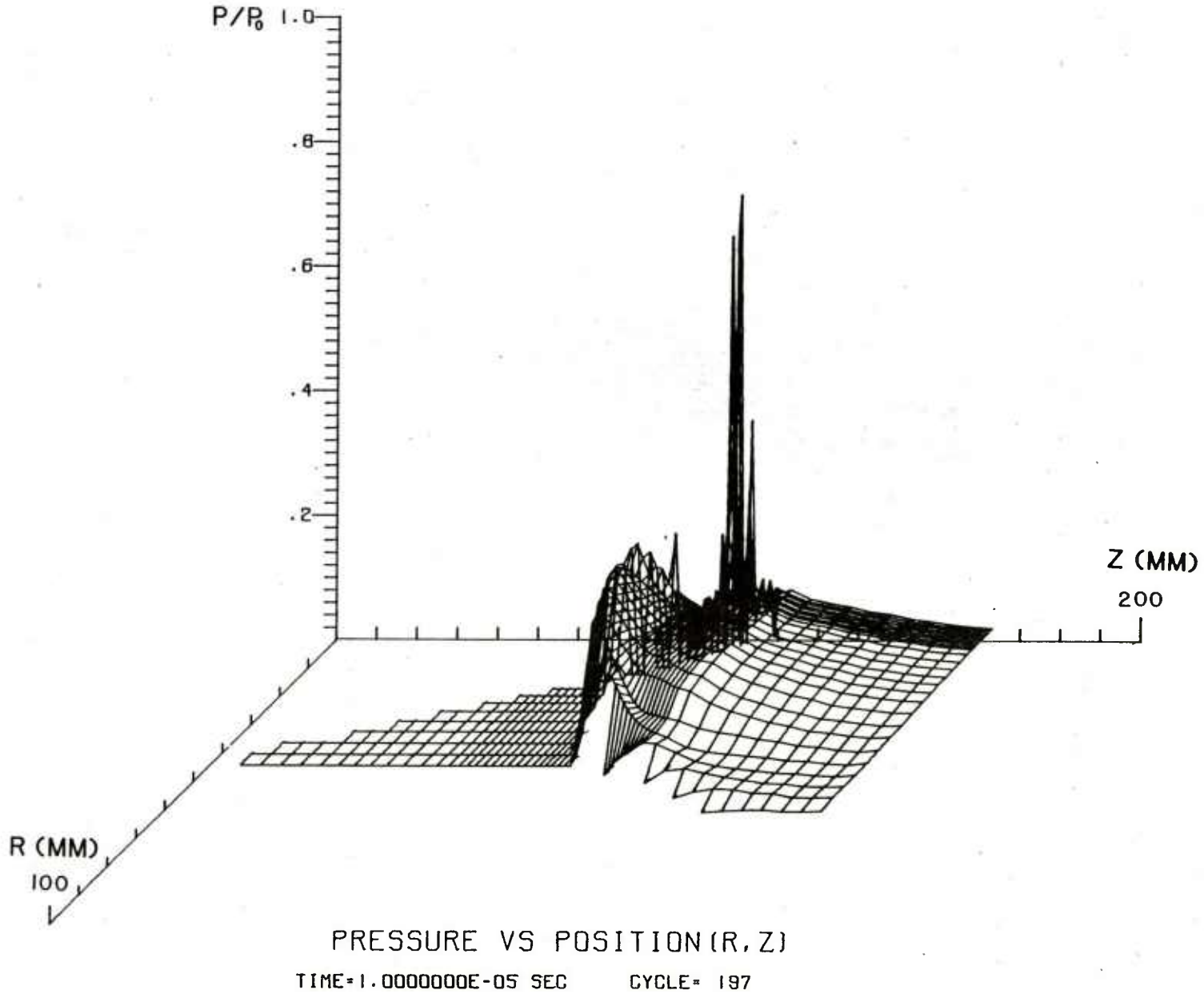

Figure 23. Three dimensional pressure field on the Eulerian grid at time = 10μs. Results from run number 4 on Table 1.

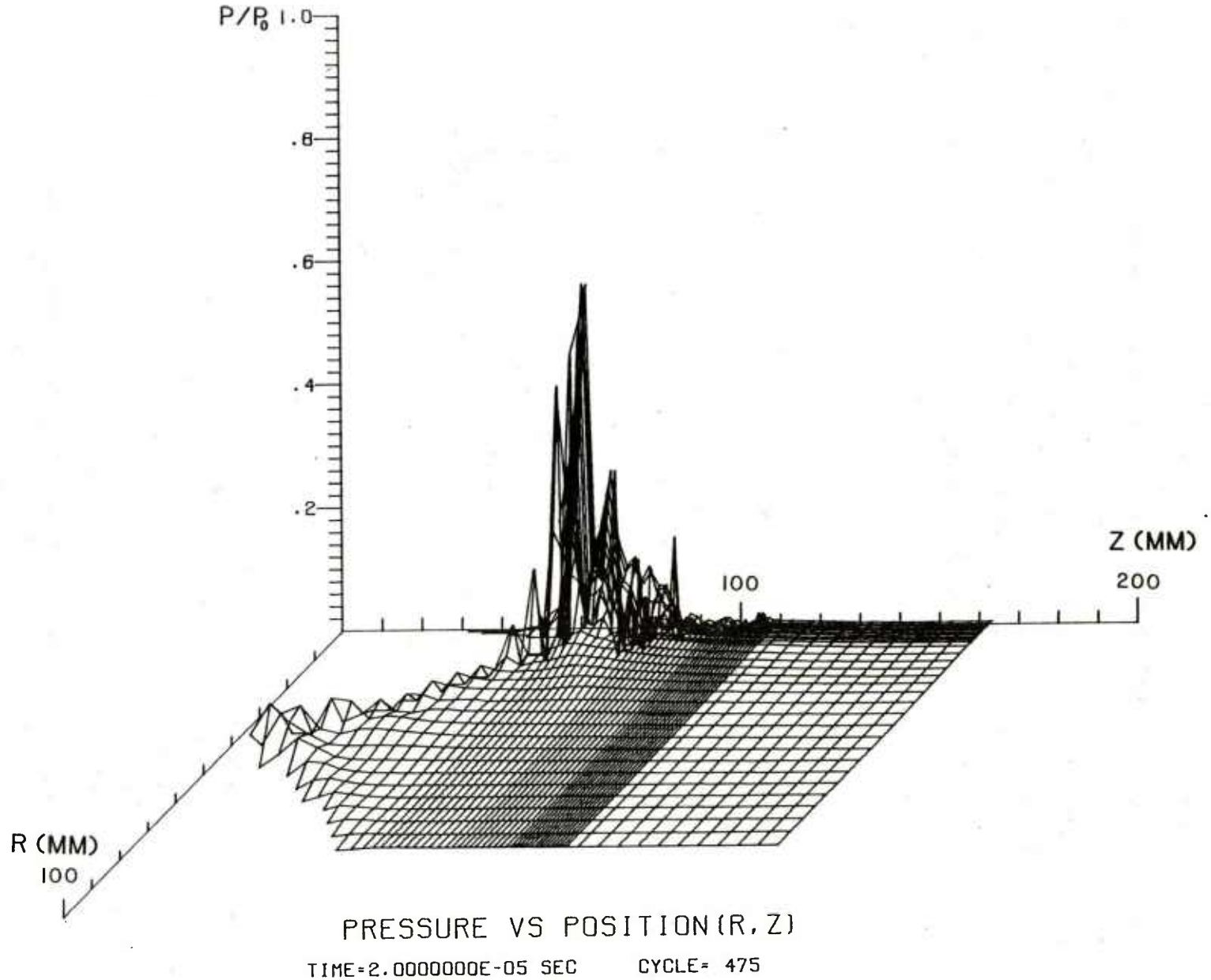

Figure 24. Three dimensional pressure field on the Eulerian grid at time = 20μs. Results from run number 4 on Table 1.

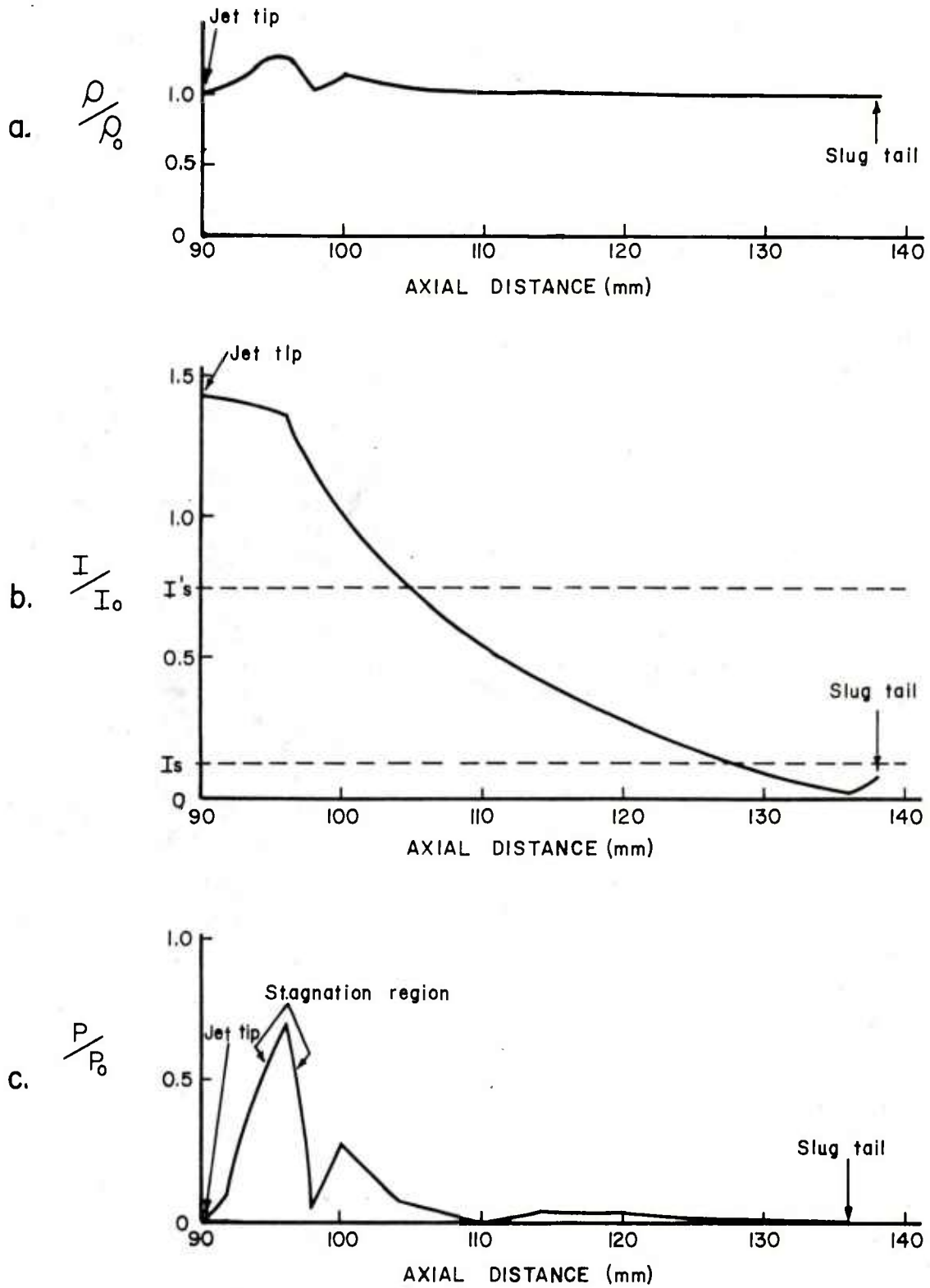

Figure 25. Detailed analysis of calculated results of the 105mm shaped charge (see number 3, on Table I), along the axis of symmetry at 20μs after initiation of the explosive.

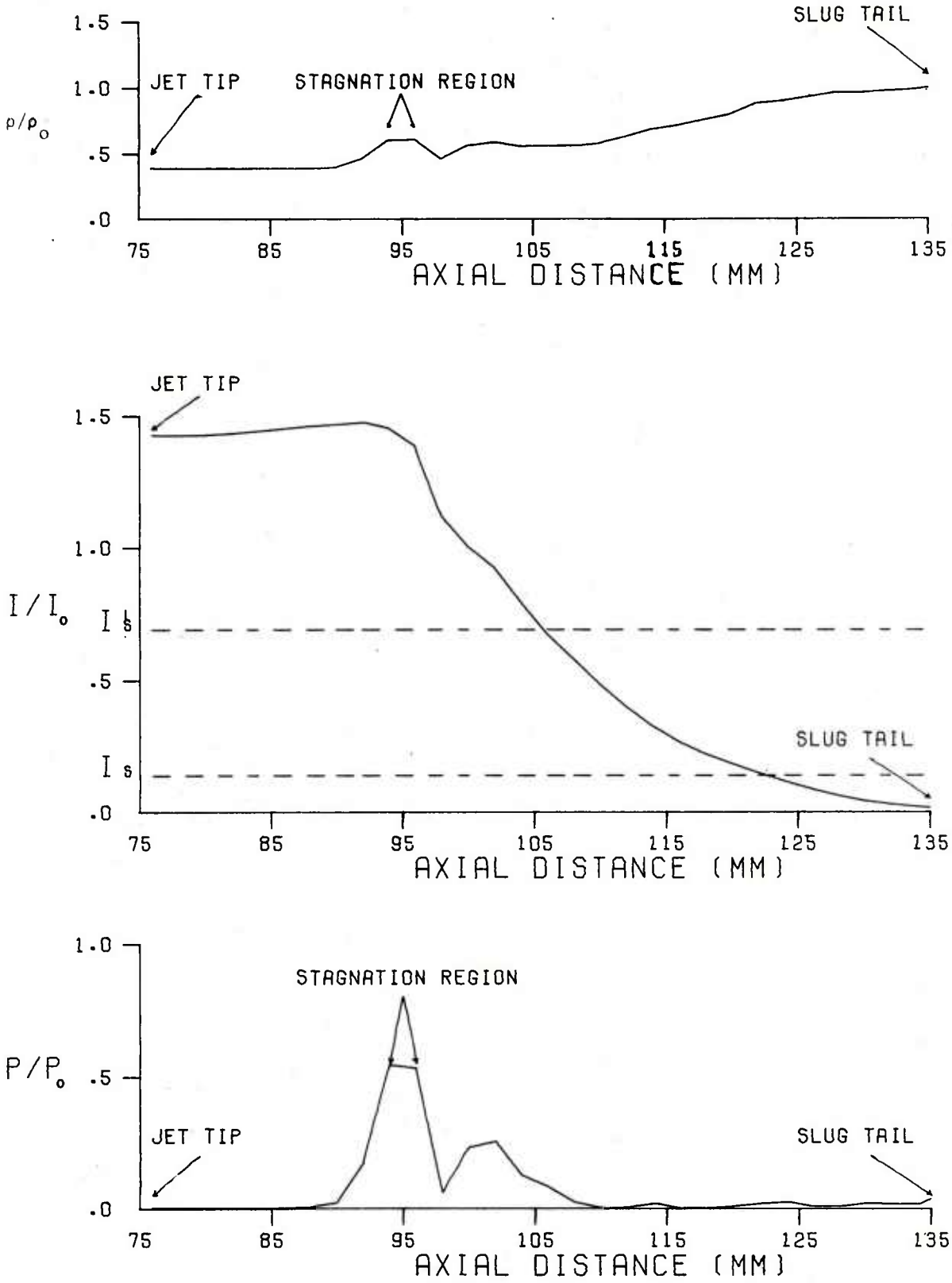

Figure 26. Detailed analysis of calculated results of the 105mm shaped charge (see number 4, on Table I), along the axis of symmetry at 20μ after initiation of the explosive

APPENDIX A

I. Equations of State for Copper Liner

There are two forms of the equation of state used for the copper liner. The first, used for determining pressures and constant energy compressibilities in the liner, is that due to J. H. Tillotson[16]. Only the condensed form of the equation of state is included since the liner material should not be shocked enough to cause significant vaporization of material. The equation of state formulations are,

for $\eta \geq 1 - \frac{A}{2B}$:

$$P = \left[a + \frac{b}{\frac{I}{I_o \eta^2} + 1} \right] I\rho + A\mu + B\mu^2 ,$$

and when $\eta < 1 - \frac{A}{2B}$

$$P = \left[a + \frac{b}{\frac{I}{I_o \eta^2} + 1} \right] I\rho - \frac{A^2}{4B}$$

In these equations P, I, and ρ are pressure, specific internal energy, and density respectively, $\eta = \frac{\rho}{\rho_o} = \mu + 1$, and the constants for the copper liner are as follows:

$a = .5$
$b = 1.5$
$A = 1.39$ Mbar
$B = 1.1$ Mbar
$I_o = .325 \times 10^5$ joules/g
$\rho_o = 8.9$ Mg/m^3

---

[16] *J. H. Tillotson, "Metallic Equations of State for Hypervelocity Impacts", General Atomic Report GS-3216, July 1961.*

The second is taken from the HEMP code report[17]. The equation-of-state formulations are,

for $\eta \geq 1 - \frac{A}{2B}$:

$$P = A\mu + B\mu^2,$$

and when $\eta < 1 - \frac{A}{2B}$:

$$P = -\frac{A^2}{4B}$$

The constants for the copper liner are as follows:

$A = 1.19$ Mbar

$B = 4.35$ Mbar

$\rho_o = 8.9$ Mg/m^3

[17] *Unpublished HEMP User's Code Report from M. Wilkens, Lawrence Radiation Laboratory.*

APPENDIX B

II. Equation of State for Composition B Explosive

There are two forms of the equation of state used for the grade A, composition B explosive. The first is a modified gamma-law equation of state of the explosive.

$$P = (\gamma - 1)\rho \quad \mathrm{MAX}[I_{min}, (I - C \cdot I_o)]$$

In this equation, P, I, and ρ are the pressure, specific internal energy, and mass density respectively. The constants for composition B explosive for γ, I_o, and ρ_o and 2.71, 5.034×10^3 joules/g, and 1.717 Mg/m^3 respectively. I_{min} is an input parameter (usually about 10^{-1} joules/g). The variable C is a flag ranging between 0 and 1 which determines whether a cell is behind (C = 0), intercepted by (0 < C < 1) or ahead (C = 1) of the detonation front. For details see report by M. L. Gittings[1].

The second uses the Jones-Wilkins-Lee[18] (JWL) equation of state for the grade A, composition B explosive.

$$P = \left[A\left(1 - \frac{a\rho}{\alpha\rho_o}\right)e^{-\frac{\alpha\rho_o}{\rho}} + B\left(1 - \frac{a\rho}{\beta\rho_o}\right)e^{-\frac{\beta\rho_o}{\rho}} + a\rho \ \mathrm{MAX}\left[I_{min}, (I - C \cdot I_o)\right]\right]$$

where: A = 5.2423 Mbar

B = .076783 Mbar

a = .34

α = 4.2

β = 1.1

I_o = 4.95×10^3 joules/g

ρ_o = 1.717 Mg/m^3

The variable C and constant I_o are used to determine the cells intercepted by the detonation front as explained above.

---

[18] *E. Lee, M. Finger, and W. Collins, "JWL Equation of State Coefficients for High Explosives," Lawrence Livermore Laboratory, UCID-16189, January 1963.*

DISTRIBUTION LIST

No. of Copies	Organization
12	Commander Defense Documentation Center ATTN: DDC-TCA Cameron Station Alexandria, VA 22314
1	Director of Defense Research and Engineering ATTN: Tech Lib, Rm 3D-1039 Washington, DC 20301
1	Director Defense Advanced Research Projects Agency ATTN: Dr. Ernest F. Blase 1400 Wilson Boulevard Arlington, VA 22209
1	Commander US Army Materiel Development and Readiness Command ATTN: DRCDMD-ST 5001 Eisenhower Avenue Alexandria, VA 22333
1	Commander US Army Aviation Research and Development Command ATTN: DRSAV-E 12th and Spruce Streets St. Louis, MO 63166
1	Director US Army Air Mobility Research and Development Laboratory Ames Research Center Moffett Field, CA 94035
1	Commander US Army Electronics Research and Development Command Technical Support Activity ATTN: DELSD-L Fort Monmouth, NJ 07703
1	Commander US Army Communications Rsch and Development Command ATTN: DRDCO-SGS Fort Monmouth, NJ 07703
3	Commander US Army Missile Research and Development ATTN: DRDMI-R Mr. W. Zecher Mr. R. Masucci Redstone Arsenal, AL 35809
1	Commander US Army Missile Materiel Readiness Command ATTN: DRSMI-AOM Redstone Arsenal, AL 35809
1	Commander US Army Tank Automotive Research & Development Cmd ATTN: DRDTA-UL Warren, MI 48090
1	Commander US Army Armament Materiel Readiness Command ATTN: DRSAR-LEP-L, Tech Lib Rock Island, IL 61299
7	Commander US Army Armament Research and Development Command ATTN: Dr. N. Clark Mr. G. Randers-Pehrson Mr. J. Pearson Mr. J. Hershkowitz Mr. A. Anzalone DRDAR-TSS (2 cys) Dover, NJ 07801

DISTRIBUTION LIST

No. of Copies	Organization
3	Commander US Army Materials and Mechanics Research Center ATTN: DRXMR-ARL, W. Woods DRXMR-T, J. Mescall Tech Lib Watertown, MA 02172
1	Director US Army TRADOC Systems Analysis Activity ATTN: ATAA-SL, Tech Lib White Sands Missile Range NM 88002
1	Assistant Secretary of the Army (R&D) ATTN: Asst for Research Washington, DC 20310
1	HQDA (DAMA-ZA; DAMA-AR) Washington, DC 20310
1	Commander US Army Research Office P. O. Box 12211 Research Triangle Park NC 27709
2	Commander Naval Air Systems Command ATTN: Code AIR-310 Code AIR-350 Washington, DC 20360
1	Commander Naval Ordnance Systems Command ATTN: Code ORD-0332 Washington, DC 20360
2	Chief of Naval Research ATTN: Code 427 Code 470 Department of the Navy Washington, DC 20325
4	Commander Naval Surface Weapons Center ATTN: Dr. H. Sternberg Mr. W. Walker Dr. J. Coughlin Code 730, Lib Silver Spring, MD 20910
2	Commander Naval Surface Weapons Center ATTN: DG-50, K. Bannister DX21, Lib Br. Dahlgren, VA 22448
1	Commander Naval Weapons Center ATTN: Code 45, Tech Lib China Lake, CA 93555
1	Commander Naval Research Laboratory Washington, DC 20375
1	USAF/AFRDDA Washington, DC 20330
1	AFSC/SDW Andrews AFB Washington, DC 20331
1	US Air Force Academy ATTN: Code FJS- RL (NC) Tech Lib Colorado Springs, CO 80840
1	AFATL/DLJW, Mr. Beech Eglin AFB, FL 32542
1	AFWL (SUL, LT Tennant) Kirtland AFB, NM 87116
1	AFAL/AVW Wright-Patterson AFB, OH 45433
1	AFLC/MMWMC Wright-Patterson AFB, OH 45433

DISTRIBUTION LIST

No. of Copies	Organization
1	Director US Bureau of Mines ATTN: Mr. R. Watson 4800 Forbes Street Pittsburgh, PA 15213
6	Director Lawrence Radiation Laboratory ATTN: Dr. M. Wilkins Dr. J. Kury E. D. Giroux Dr. E. Lee Dr. H. Horning Tech Lib P. O. Box 808 Livermore, CA 94550
1	Director National Aeronautics and Space Administration Langley Research Center Langley Station Hampton, VA 23365
1	Director National Aeronautics and Space Administration Lewis Research Center 21000 Brookpark Road Cleveland, OH 44135
1	Lockheed Missiles and Space Company ATTN: Mr. J. E. May 55-80 Bldg. 57 P. O. Box 504 Sunnyvale, CA 94088
1	Computer Code Consultants ATTN: Mr. W. Johnson 527 Glencrest Drive Solana Beach, CA 92075
1	Physics International Corp ATTN: Mr. L. Behrmann 2700 Merced Street San Leandro, CA 94577
2	Sandia Laboratories ATTN: Dr. W. Herrman Dr. L. Bertholf Albuquerque, NM 87115
1	Shock Hydrodynamics ATTN: Dr. L. Zernow 4710-4716 Vineland Avenue North Hollywood, CA 91602
1	Systems, Science & Software ATTN: Dr. R. Sedgwick P. O. Box 1620 La Jolla, CA 92037
2	Drexel Institute of Technology Wave Propagation Research Ctr ATTN: Prof. P. Chou Dr. J. Carleone 32nd & Chestnut Streets Philadelphia, PA 19104
1	Stanford Research Institute ATTN: Dr. A. Florence Poulter Laboratories Menlo Park, CA 94025
3	University of California Los Alamos Scientific Lab ATTN: Dr. R. Karpp Dr. J. Walsh Tech Lib P. O. Box 1663 Los Alamos, NM 87545

DISTRIBUTION LIST

No. of Copies	Organization
1	Washington State University Department of Physics ATTN: Prof. G. Duvall Pullman, WA 99163

Aberdeen Proving Ground

Dir, USAMSAA
Cdr, USATECOM
ATTN: DRSTE-SG-H